

**Electronic Supporting Information**

**Solvent and additive-free efficient aerobic oxidation of alcohols by perovskite oxide based heterogeneous catalyst**

**Nikhil Kumar,<sup>a</sup> Kumari Naveen,<sup>a</sup> Anita Bhatia,<sup>a</sup> Senthilkumar Muthaiah,<sup>a</sup> Vasudeva Siruguri,<sup>b</sup> and Avijit Kumar Paul<sup>a\*</sup>**

*<sup>a</sup>Department of Chemistry, National Institute of Technology, Kurukshetra-136119, Haryana, India.*

*<sup>b</sup>UGC-DAE Consortium for Scientific Research Mumbai Centre, 246-C CFB, BARC Campus, Mumbai – 400085, India.*

**Table of Contents:**

**1. Experimental section**

**2. Tables**

**3. Figures**

**4. References**

## Experimental section:

### XANES study:

The beamline optics consists of Rh/Pt coated collimating meridional cylindrical mirror and the collimated beam reflected by the mirror monochromatized by a Si (111) ( $2d = 6.2709 \text{ \AA}$ ) based double crystal monochromator (DCM). The second crystal of DCM is a sagittal cylinder used for horizontal focusing while a Rh/Pt coated bendable post mirror facing down is used for vertical focusing of the beam at the sample position. In the present case, XAS measurements have been performed in transmission mode. For the transmission measurement, three ionization chambers (300 mm length each) have been used for data collection, one ionization chamber for measuring incident flux ( $I_0$ ), second one for measuring transmitted flux ( $I_t$ ) and the third ionization chamber for measuring spectrum of a reference metal foil for energy calibration. Appropriate gas pressure and gas mixtures have been chosen to achieve 10-20% absorption in first ionization chamber and 70-90% absorption in second ionization chamber to improve the signal to noise ratio. The absorption coefficient  $\mu$  is obtained using the relation:

$$I_T = I_0 e^{-\mu x} \quad (2)$$

where,  $x$  is the thickness of the absorber,  $I_0$  and  $I_T$  are incident and the transmitted flux, respectively. The normalised XANES spectra at Ru-K edge is shown in Figure S6a along with reference spectra of Ru+3, Ru+4 and Ru+5 oxidation states. As it can be seen from Figure S6a, the absorption edge position of CLSR is in between +4 and +5 oxide samples. The linear combination fitting (LCF) is done to know the qualitative ratio of different oxidation state in the sample. It is found from the LCF analysis that CLSR is contribution of 94% of +5 and 6% of +4 oxidation states and no trace is found for +3 oxidation state.<sup>1,2</sup>

### H<sub>2</sub>-TPR:

285 mg of CLSR pre-treated at 150°C in highly pure helium Gas (25cc/min) for 1 hour. After cooling to room temperature in helium gas, the inlet gas was changed to 5% H<sub>2</sub>/Ar (25cc/min) at room temp and waited till baseline is stable. Then, TPR experiment was started from RT to 850°C at the heating rate of 10 °C/min. The variation of H<sub>2</sub> concentration in the outlet gas was continuously monitored by a TCD detector.<sup>3,4</sup>

## Spectral data of products:

**Acetophenone (1a):** Colourless, viscous liquid, isolated yield: 0.05391 mL, 91%. <sup>1</sup>H-NMR (400 MHz, CDCl<sub>3</sub>, TMS), δ ppm: 7.96- 7.94 (m, 2H, Ar), 7.57-7.55 (m, 1H, Ar), 7.49-7.45 (m, 2H, Ar), 2.59 (s, 3H, CH<sub>3</sub>).<sup>5</sup>

**1-(4-methylphenyl) ethanone (1b):** Isolated yield: 86%. <sup>1</sup>H-NMR (400 MHz, CDCl<sub>3</sub>, TMS), δ ppm: 2.42 (s, 3H, CH<sub>3</sub>), 2.59 (s, 3H, CH<sub>3</sub>), 7.28-7.26 (m, 2H, Ar), 7.88-7.86 (m, 2H, Ar).<sup>6</sup>

**1-(4-Methoxyphenyl) ethanone (1c):** Isolated yield: 85%. <sup>1</sup>H-NMR (400 MHz, CDCl<sub>3</sub>, TMS), δ ppm: 2.56 (s, 3H, CH<sub>3</sub>), 3.87 (s, 3H, CH<sub>3</sub>), 6.96–6.94 (m, 2H, Ar), 7.97–7.94 (m, 2H, Ar).<sup>6</sup>

**1-(4-Chlorophenyl) ethanone (1d):** Isolated yield: 88%.  $^1\text{H-NMR}$  (400 MHz,  $\text{CDCl}_3$ , TMS),  $\delta$  ppm: 2.54 (s, 3H,  $\text{CH}_3$ ), 7.39-7.37 (d, 2H, Ar), 7.86- 7.83 (d, 2H, Ar).<sup>6</sup>

**1-(4-Bromophenyl) ethanone (1e):** Isolated yield: 89%.  $^1\text{H-NMR}$  (400 MHz,  $\text{CDCl}_3$ , TMS),  $\delta$  ppm: 2.61 (s, 3H,  $\text{CH}_3$ ), 7.64-7.62 (m, 2H, Ar), 7.85-7.83 (m, 2H, Ar).<sup>5</sup>

**1-(4-Nitrophenyl) ethanone (1f):** Isolated yield: 85%.  $^1\text{H-NMR}$  (400 MHz,  $\text{CDCl}_3$ , TMS),  $\delta$  ppm: 2.69 (s, 3H,  $\text{CH}_3$ ), 8.13-8.11 (m, 2H, Ar), 8.32-8.30 (m, 2H, Ar).<sup>5</sup>

**Cyclohexanone (1g):** Isolated yield: 87%.  $^1\text{H-NMR}$  (400 MHz,  $\text{CDCl}_3$ , TMS),  $\delta$  ppm: 2.27-2.24 (t, 2H,  $\text{CH}_2$ ), 1.80-1.77 (m, 2H,  $\text{CH}_2$ ), 1.66-1.64 (m, 1H, CH).<sup>6</sup>

**3-methyl-2-butanone (1h):** Isolated yield: 84%.  $^1\text{H-NMR}$  (400 MHz,  $\text{CDCl}_3$ , TMS),  $\delta$  ppm: 1.09-1.07 (d, 6H,  $\text{CH}_3$ ), 2.12 (s, 3H,  $\text{CH}_3$ ), 2.59-2.55 (m, 1H, CH).<sup>5</sup>

**Benzophenone (1i):** Isolated yield: 90%.  $^1\text{H-NMR}$  (400 MHz,  $\text{CDCl}_3$ , TMS),  $\delta$  ppm: 7.52-7.48 (m, 4H, Ar), 7.63-7.59 (m, 2H, Ar), 7.84-7.82 (m, 4H, Ar).<sup>5</sup>

**Benzaldehyde (2a):** Colourless, liquid, isolated yield: 0.0352 mL, 71%.  $^1\text{H-NMR}$  (400 MHz,  $\text{CDCl}_3$ , TMS),  $\delta$  ppm: 7.91- 7.87 (m, 2H, Ar), 7.67-7.62 (m, 1H, Ar), 7.59-7.52 (m, 2H, Ar), 10.0-10.03 (s, 1H, CHO).<sup>6</sup>

**4-Fluoro Benzaldehyde (2b):** Isolated yield: 74%.  $^1\text{H-NMR}$  (400 MHz,  $\text{CDCl}_3$ , TMS),  $\delta$  ppm: 7.24-7.20 (d, 2H, Ar), 8.15-7.90 (d, 2H, Ar), 9.97(s, 1H, CHO).<sup>5</sup>

**4-Chloro Benzaldehyde (2c):** Isolated yield: 78%.  $^1\text{H-NMR}$  (400 MHz,  $\text{CDCl}_3$ , TMS),  $\delta$  ppm: 7.54-7.52 (d, 2H, Ar), 7.85-7.83 (d, 2H, Ar), 10.00 (s, 1H, CHO).<sup>5</sup>

**4-Bromo Benzaldehyde (2d):** Isolated yield: 80%.  $^1\text{H-NMR}$  (400 MHz,  $\text{CDCl}_3$ , TMS),  $\delta$  ppm: 7.5-7.39 (d, 2H, Ar), 7.9-7.88 (d, 2H, Ar), 10.43 (s, 1H, CHO).<sup>6</sup>

**4-Methoxy Benzaldehyde (2e):** Isolated yield: 80%.  $^1\text{H-NMR}$  (400 MHz,  $\text{CDCl}_3$ , TMS),  $\delta$  ppm: 3.88 (s, 3H,  $\text{CH}_3$ ), 7.0-6.98 (d, 2H, Ar), 7.84-7.82 (d, 2H, Ar), 9.87 (s, 1H, CHO).<sup>6</sup>

**2-Chloro Benzaldehyde (2f):** Isolated yield: 76%.  $^1\text{H-NMR}$  (400 MHz,  $\text{CDCl}_3$ , TMS),  $\delta$  ppm: 7.9-7.87 (s, 1H, Ar), 7.5-7.35 (m, 3H, Ar), 10.44 (s, 1H, CHO).<sup>5</sup>

**2,4-di chloro Benzaldehyde (2g):** Isolated yield: 74%.  $^1\text{H-NMR}$  (400 MHz,  $\text{CDCl}_3$ , TMS),  $\delta$  ppm: 7.86-7.84 (s, 1H, Ar), 7.55-7.53 (d, 2H, Ar), 10.01 (s, 1H, CHO).<sup>5</sup>

**$\gamma$ -Butyrolactone(3a):** Isolated Yield: 53%,  $^1\text{H NMR}$  (400 MHz,  $\text{CDCl}_3$ )  $\delta$  2.19 (m, 2 H), 2.51(t, 2H), 4.36 (t, 2H).<sup>7</sup>

**$\beta$ -Propiolactone (3b):** Isolated Yield: 45%,  $^1\text{H NMR}$  (400 MHz,  $\text{CDCl}_3$ )  $\delta$  3.55 (t, 2H), 4.29 (t, 2H).<sup>7</sup>

**$\delta$ -Valerolactone (3c):** Isolated Yield: 57%,  $^1\text{H NMR}$  (400 MHz,  $\text{CDCl}_3$ )  $\delta$  1.92-2.02 (m, 2H), 2.64 (t, 1H), 4.36 (t, 1H).<sup>7</sup>

**$\gamma$ -Valerolactone (3d):** Isolated Yield: 60%,  $^1\text{H NMR}$  (400 MHz,  $\text{CDCl}_3$ )  $\delta$  1.62 (d, 3H), 1.92-1.95 (m, 1H), 2.17 (m, 1H), 2.47-2.56 (m, 2H), 4.42-4.47 (m, 1H).<sup>7</sup>

**4-methyltetrahydro-2H-pyran-2-one (3e):** Isolated Yield: 56%,  $^1\text{H NMR}$  (400 MHz,  $\text{CDCl}_3$ )  $\delta$  1.09 (d, 3H), 1.65-2.51(m, 5H), 4.29-4.42 (m, 2H).<sup>7</sup>

**Isobenzofuran-1(3H)-one (3f):** Isolated Yield: 58%,  $^1\text{H NMR}$  (400 MHz,  $\text{CDCl}_3$ )  $\delta$  5.53 (s, 2 H), 7.31(m, 2H), 7.47 (m, 1H), 7.79 (m, 1H).<sup>7</sup>

**2-Chromanone (3g):** Isolated Yield: 54%,  $^1\text{H NMR}$  (400 MHz,  $\text{CDCl}_3$ )  $\delta$  2.67 (t, 2H), 2.90 (t, 2H), 7.09-7.22 (m, 4H).<sup>7</sup>

## Tables:

**Table. S1:** Results of the crystal structure refinements for CLSR ( $\text{CaLaScRuO}_{6.10}$ ) as obtained from room temperature NPD and PXRD. The crystal structure refined in the orthorhombic space group  $Pnma$ .

Refinement parameters	<b>NPD</b>	<b>PXRD</b>
$T$ [K]	$RT$	$RT$
Space group	$Pnma$	$Pnma$
$a$ [\AA]	5.6402 (2)	5.6524 (5)
$b$ [\AA]	7.9077 (2)	7.9092 (7)
$c$ [\AA]	5.5579 (2)	5.5590 (5)
$V$ [\AA <sup>3</sup> ]	247.89 (1)	248.52 (4)
$x$ (Ca/La)	0.0418 (3)	0.0377 (2)
$y$ (Ca/La)	0.25	0.25
$z$ (Ca/La)	-0.0099 (7)	-0.0055 (7)
$U_{iso}$ (Ca/La) [\AA <sup>2</sup> ]	0.00 (9)	0.0419(5)
$Occ.$ (Ca/La)	0.5/0.5	0.5/0.5
$x$ (O1)	0.2962 (3)	0.2737 (11)
$y$ (O1)	0.0461 (3)	0.0569 (8)
$z$ (O1)	0.7050 (3)	0.7112 (11)
$U_{iso}$ (O1) [\AA <sup>2</sup> ]	0.00 (9)	0.0000 (19)
$Occ.$ (O1)	2.05	2.05
$x$ (O2)	0.4705 (4)	0.4680 (14)
$y$ (O2)	0.25	0.25
$z$ (O2)	0.0862 (6)	0.072 (2)
$U_{iso}$ (O2) [\AA <sup>2</sup> ]	0.00 (9)	0.029(4)
$Occ.$ (O2)	1.0	1.0
$R_F$	1.69	3.51
$R_{Bragg}$	3.03	1.80
$R_P$	2.67	2.79
$R_{exp}$	1.80	1.59
$R_{wp}$	3.46	4.57
$\chi^2$	3.69	8.25
$d_{eq}$ (Sc/Ru-O'1) [\AA]	2.0353 (17)	1.9936 (62)
$d_{eq}$ (Sc/Ru-O1) [\AA]	2.0548 (17)	2.1015 (62)
$d_{ax}$ (Sc/Ru-O2) [\AA]	2.409 (8)	2.0255 (23)
O1-Sc/Ru-O1	180.0	180.0
Sc/Ru-O'1-Sc/Ru	150.939 (21)	150.918 (33)

Sc/Ru-O2-Sc/Ru	151.223 (1)	154.952 (2)
	<i>B</i> -site (Sc/Ru) are at special positions ( $x=0, y=0, z=0.5$ ), $U_{iso} = 0.00(9)$ , Occ. (Sc/Ru) = 0.5/0.5.	<i>B</i> -site (Sc/Ru) are at special positions ( $x=0, y=0, z=0.5$ ), $U_{iso} = 0.0255(5)$ , Occ. (Sc/Ru) = 0.5/0.5

**Table S2:** Selected bond length and bond angles from room temperature NPD refinement of CLSR.

Bond length	[Å]	Bond angle	[°]
Ca/La-O1	2.7828 (28)	Sc/Ru-O'1-Sc/Ru	150.939 (91)
Ca/La-O'1	2.3863 (29)	Sc/Ru-O2-Sc/Ru	151.223 (1)
Ca/La-O''1	2.6776 (32)	O1-Sc/Ru-O1	180
Ca/La-O2	2.3890 (51)	O1-Sc/Ru-O'1	88.896 (67)
Ca/La-O'2	2.4763 (30)	O1-Sc/Ru-O2	91.744 (65)
Sc/Ru-O'1	2.0353 (17)	O'1-Sc/Ru-O2	88.591 (64)
Sc/Ru-O1	2.0548 (17)	Sc/Ru-O1-Ca/La	90.550 (64)
Sc/Ru-O2	2.409 (8)	Sc/Ru-O'1-Ca/La	89.958 (64)
O'1-O2	2.9259 (27)	Sc/Ru-O2-Ca/La	102.572 (1)
O1-O'1	2.8641 (24)		
O1-O2	2.9315 (30)		

**Table S3:** Isolated and % GC yield of carbonyl compounds observed after 6 hours of each reaction.

Entry	Compound	Isolated yield <sup>a</sup> & %	% GC Yield <sup>b</sup> (TON, TOF in h <sup>-1</sup> ) <sup>c</sup>
1		0.05391 mL & 92%	96 (96, 16)
2		0.03969 mL & 80%	83 (83, 13.8)
3		0.0315 mL & 58%	63 (63, 10.5)

<sup>a</sup>Isolated yield average of at least two runs.

<sup>b</sup>GC yield using N-dodecane as internal standard and average of at least two runs.

<sup>c</sup>TON is calculated as the amount of reactant (in moles) divided by the amount of active catalyst (in moles) times the percentage of yield of product (in decimals, i.e. 96% is taken as 96/100). In other way, we can say as moles of converted substrate / moles of catalytic specie in the reaction.

So,  $TON = (\text{No. of moles of reactants}/\text{No. of moles of catalyst}) \times (\text{percentage yield of the product})$

$TOF = TON/\text{time}$

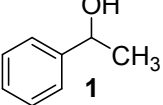
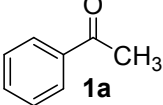
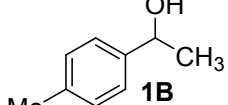
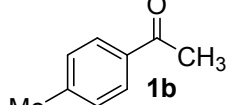
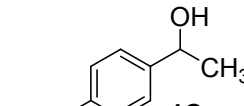
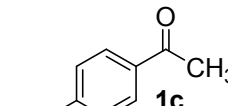
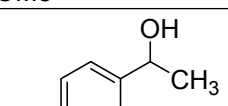
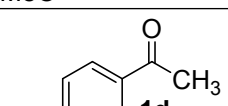
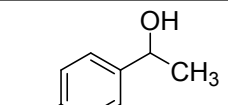
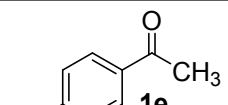
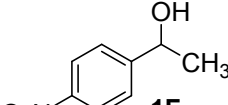
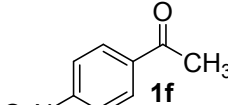
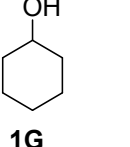
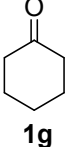
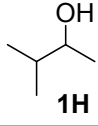
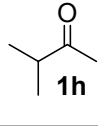
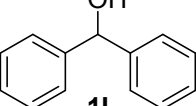
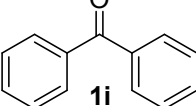
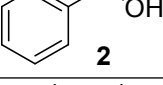
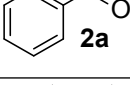
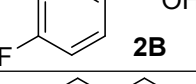
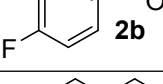
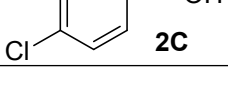
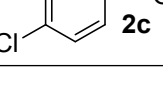
Our reactant was 0.5 mmol, catalyst was 0.005 mmol and the yield was 96% after 6 hours in Entry 1. So,  $TON = (0.5/0.005) \times (96/100) = 96$ ; and  $TOF = 96/6 = 16 \text{ h}^{-1}$ .

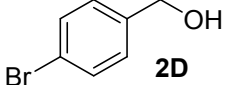
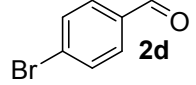
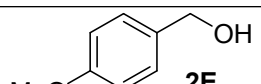
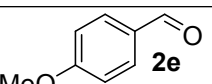
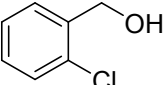
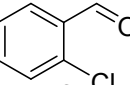
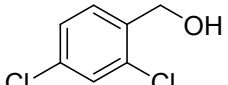
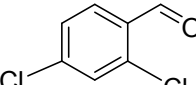
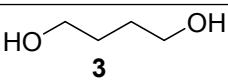
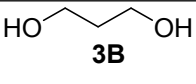
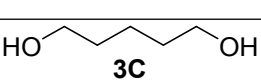
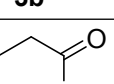
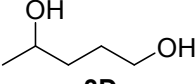
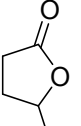
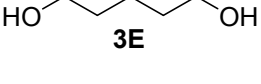
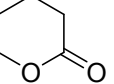
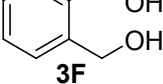
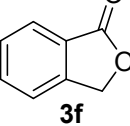
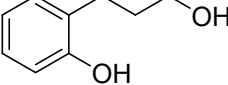
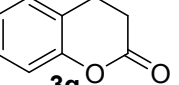
**Table S4:** The calculation of TON and TOF values for the optimization reaction of the secondary alcohol as supplied in Table 1.

Entry	Catalyst mol %	Time (h)	% GC Yield	Turnover number (TON)	Turnover frequency (TOF in h <sup>-1</sup> )
1	5	24	96	$(0.5/0.025) \times (96/100) = 19$	$19/24 = 0.79$
2	1	24	96	$(0.5/0.005) \times (96/100) = 96$	$96/24 = 4$
3	1	12	96	$(0.5/0.005) \times (96/100) = 96$	$96/12 = 8$
4	1	6	96	$(0.5/0.005) \times (96/100) = 96$	$96/6 = 16$
5	1	24	96	$(0.5/0.005) \times (96/100) = 96$	$96/24 = 4$
6	1	12	96	$(0.5/0.005) \times (96/100) = 96$	$96/12 = 8$
7	1	6	96	$(0.5/0.005) \times (96/100) = 96$	$96/6 = 16$
8	1	5.5	91	$(0.5/0.005) \times (91/100) = 91$	$91/5.5 = 16.5$
9	Nil	6	trace	trace	
10	1	6	78	$(0.5/0.005) \times (78/100) = 78$	$78/6 = 13$
11	1	6	06	06	
12	0.5	6	65	$(0.5/0.0025) \times (65/100) = 130$	$130/6 = 21.7$
13	1	6	trace	trace	

In case of 1 mol % catalyst, reactant was 0.5 mmol and catalyst was 0.005 mmol.  
In case of 5 mol % catalyst, catalyst was 0.025 mmol along with the same amount of reactant (0.5 mmol)

**Table S5:** Oxidation of primary, secondary alcohols and diols into carbonyl and lactones catalyzed by CLSR.

Entry	Substrate	Product	Isolated Yields (%)
1			92
2			86
3			85
4			88
5			89
6			85
7			87
8			84
9			92
10			80
11			74
12			78

13			80
14			80
15			76
16			74
17			58
18			50
19			62
20			65
21			61
22			63
23			59

Reaction conditions: 1 mol% catalyst, 80°C, 6 h & solvent-free.

**Table S6:** Recyclability test of catalyst (CLSR) up to 4 consecutive cycles<sup>a</sup>.

Cycle No.	1	2	3	4
% GC Yield <sup>b</sup>	96	90	86	83

<sup>a</sup>Temperature = 80 °C, Time = 6 h, Solvent free, 1mol% of catalyst for each run. <sup>b</sup>GC yield using N-dodecane as internal standard and average of at least two runs.

**Table S7:** Comparison of % GC yield of product resulted by given catalyst and metal oxides/carbonates of starting materials.

Entry	Catalyst	Reaction conditions	% GC Yield <sup>b</sup>
1.	CLSR	Optimized condition <sup>a</sup>	96
2.	CaCO <sub>3</sub>	-do-	29
3.	La <sub>2</sub> O <sub>3</sub>	-do-	50
4.	Sc <sub>2</sub> O <sub>3</sub>	-do-	14
5.	RuO <sub>2</sub>	-do-	19

<sup>a</sup>Temperature = 80 °C, Time = 6 h, Solvent free, 1mol% of catalyst.

<sup>b</sup>GC yield using N-dodecane as internal standard and average of at least two runs.

**Table S8:** Comparison of present catalyst (CLSR) with already reported catalysts containing perovskites related structures.

Entry	Catalytic material	Conditions	References
1.	CLSR	Solvent-free, additive free, 80 °C and 6 h	Present work
2.	LaMO <sub>3</sub> (M = Cr, Mn, Co, Ni, Fe)	Solvent-free, 70% TBHP, 90 °C and 0.5 h	25
3.	La <sub>1-x</sub> Ce <sub>x</sub> CoO <sub>3</sub>	Toluene, O <sub>2</sub> flow (50 mL/min), 88 °C and 1 h	23
4.	Cu loaded LaFeO <sub>3</sub>	Acetonitrile, TBHP, 80 °C, 1tm and 3 h	24
5.	LaCoO <sub>3</sub>	CCl <sub>4</sub> , 70% TBHP, Bu <sub>4</sub> N <sup>+</sup> Br <sup>-</sup> , reflux and 6 h	37
6.	CeCrO <sub>3</sub>	DMSO, 70% TBHP, 90 °C and 10 h	38
7.	SrMnO <sub>3</sub>	Toluene, 60 °C and 6 h	39
8.	RuO <sub>2</sub> supported Mn <sub>3</sub> O <sub>4</sub>	Toluene, O <sub>2</sub> /air flow (10 mL/min), 90 °C and 12 h	11
9.	Zn-Co LDH	Acetonitrile, TBHP, 65 °C and 6 h	29

**Figures:**

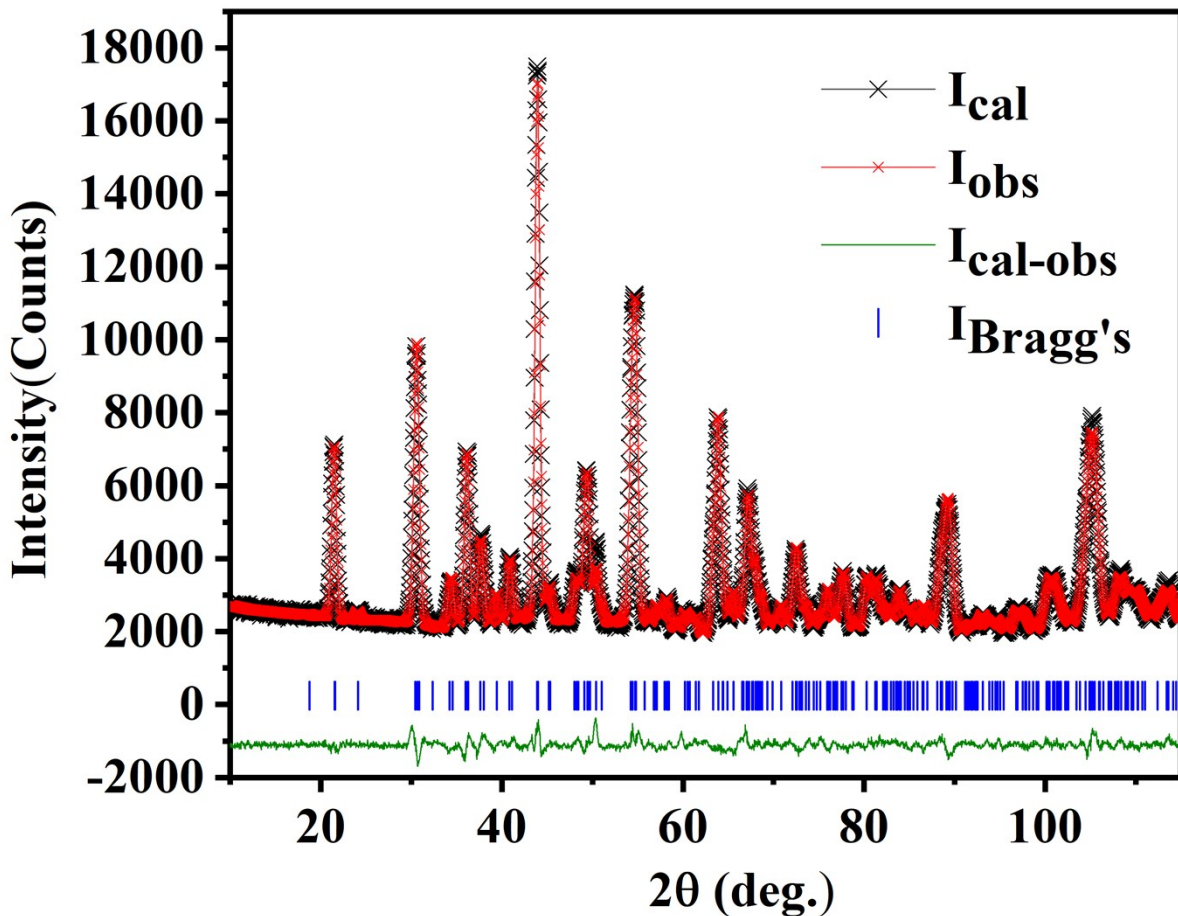


**Figure S1:** Rietveld refinement of room temperature neutron powder diffraction (NPD) pattern of CLSR catalyst.

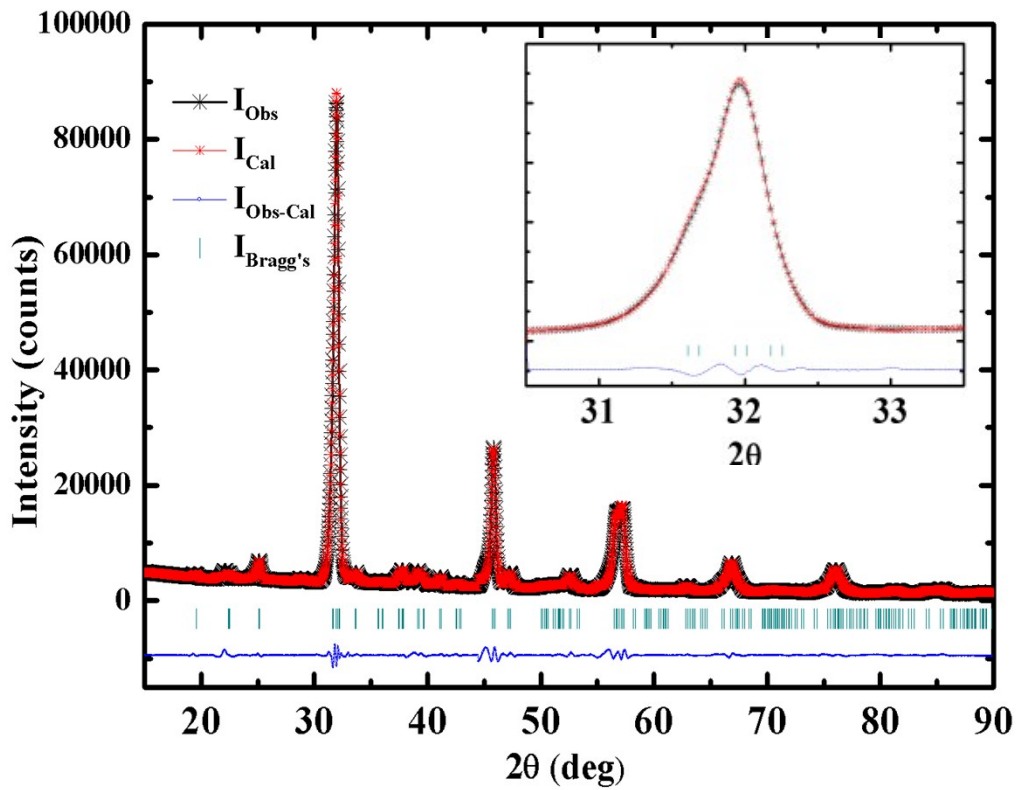


**Figure S2:** Rietveld refinement of room temperature PXRD pattern and zoom part for highest intensity peak (inset).

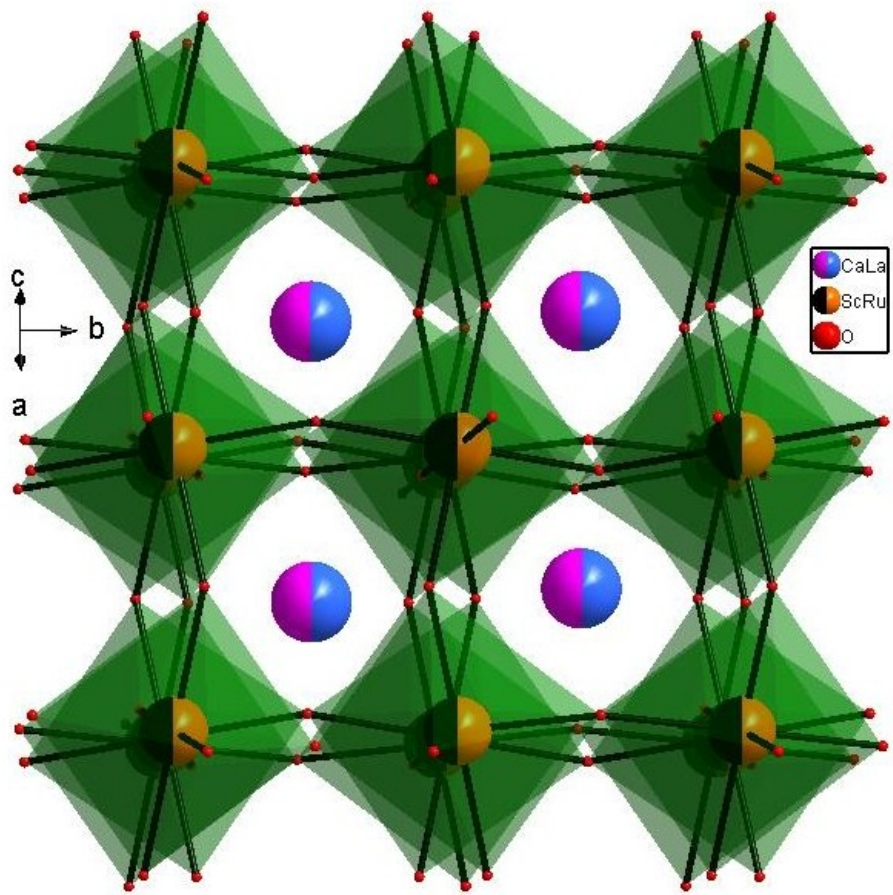


**Figure S3:** The elucidate refined crystal structure having all the four metal ions with octahedral sites.

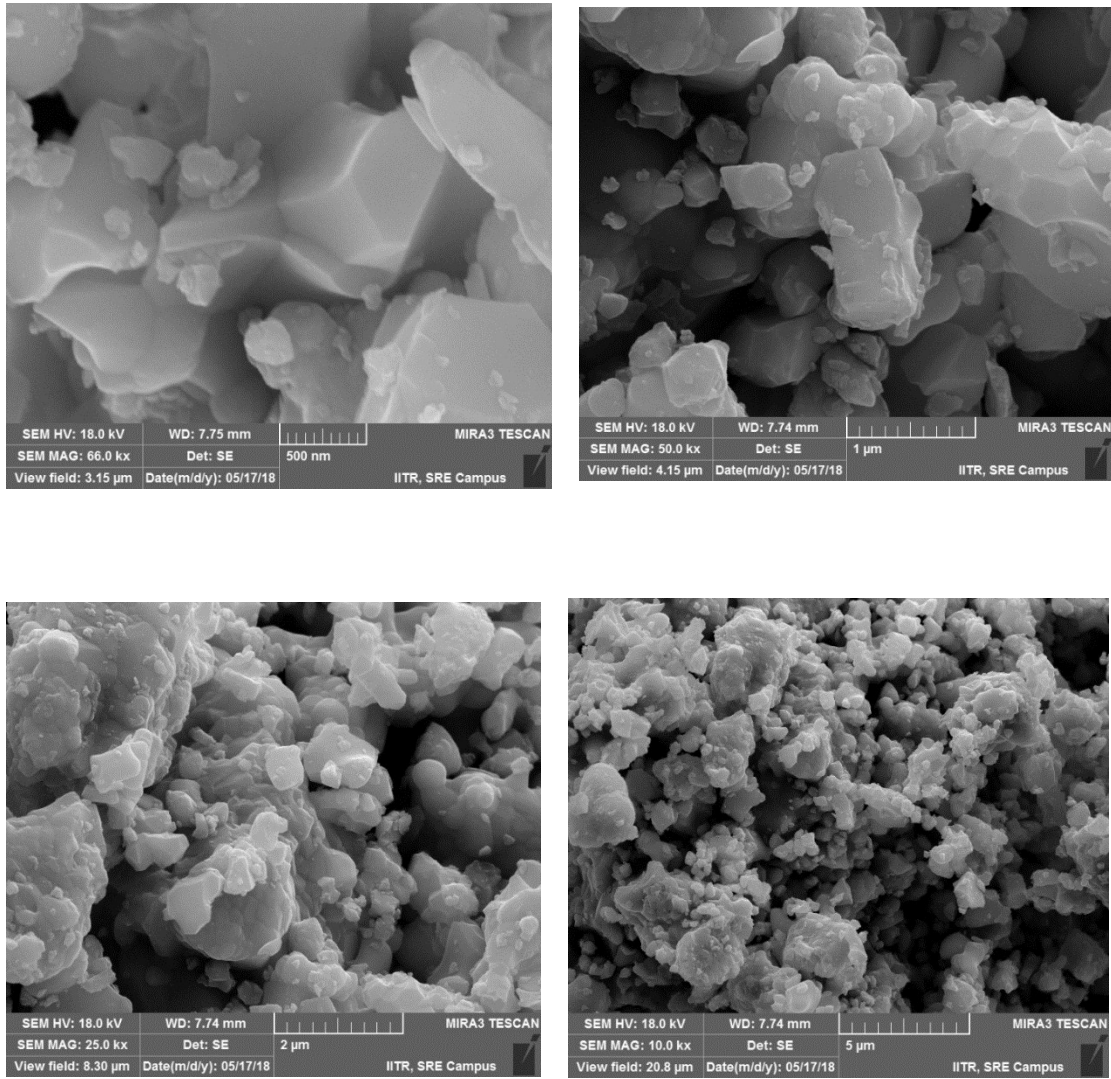
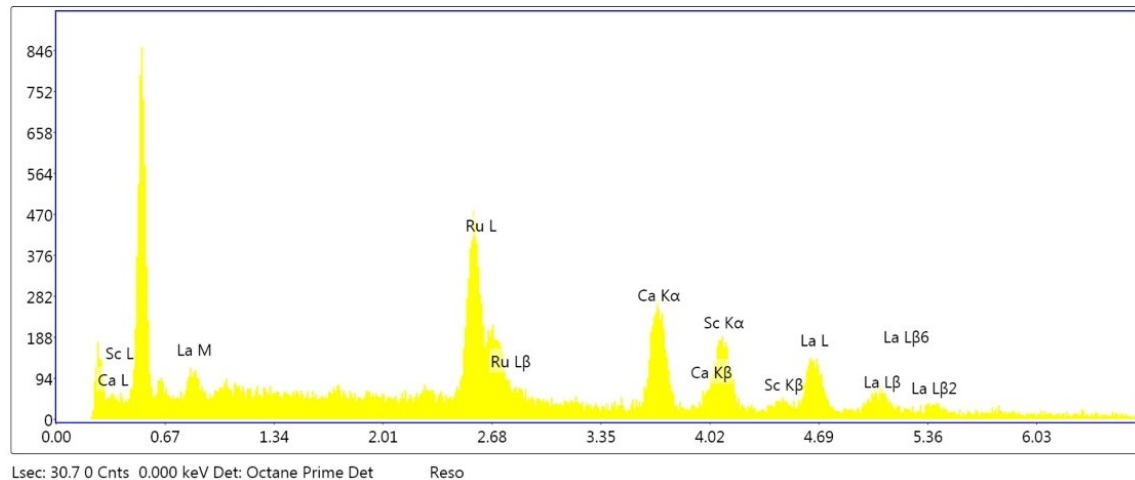
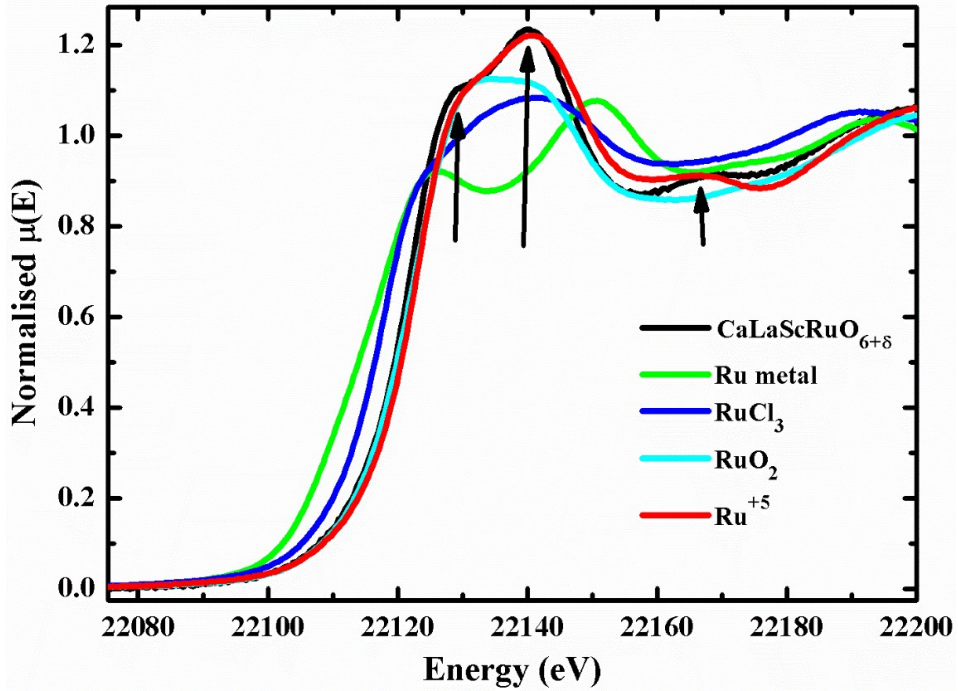


**Figure S4:** FESEM images of polycrystalline bulk material CLSR.



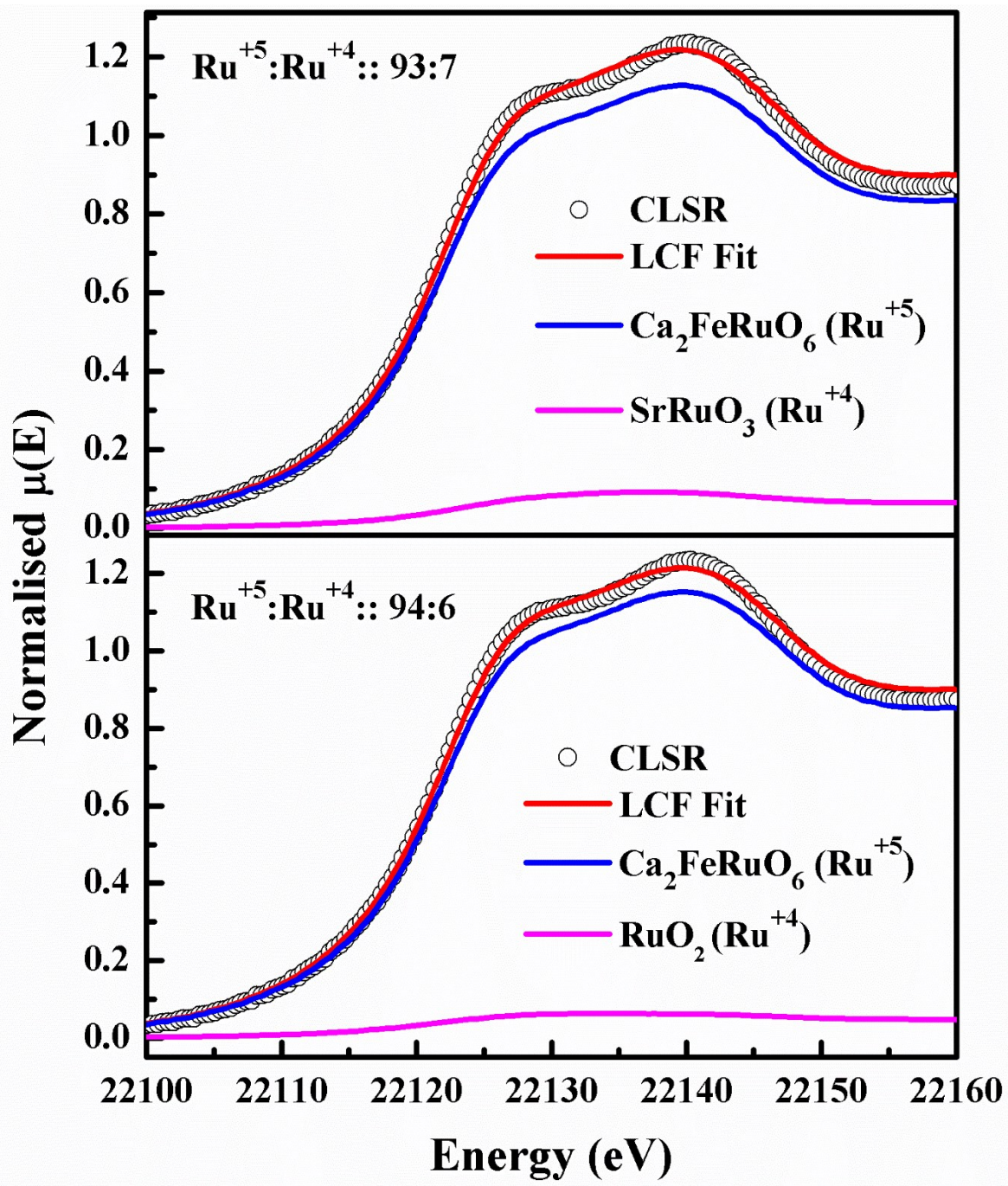
<b>Element</b>	<b>EDAX (%)</b>	<b>ICP-AES (%)</b>
<b>Ru</b>	<b>25.82</b>	<b>25.22</b>
<b>Ca</b>	<b>26.13</b>	<b>25.51</b>
<b>Sc</b>	<b>24.73</b>	<b>24.85</b>
<b>La</b>	<b>23.33</b>	<b>24.42</b>

**Figure S5:** EDAX spectra and percentage composition along with ICP-AES of polycrystalline bulk material CLSR.

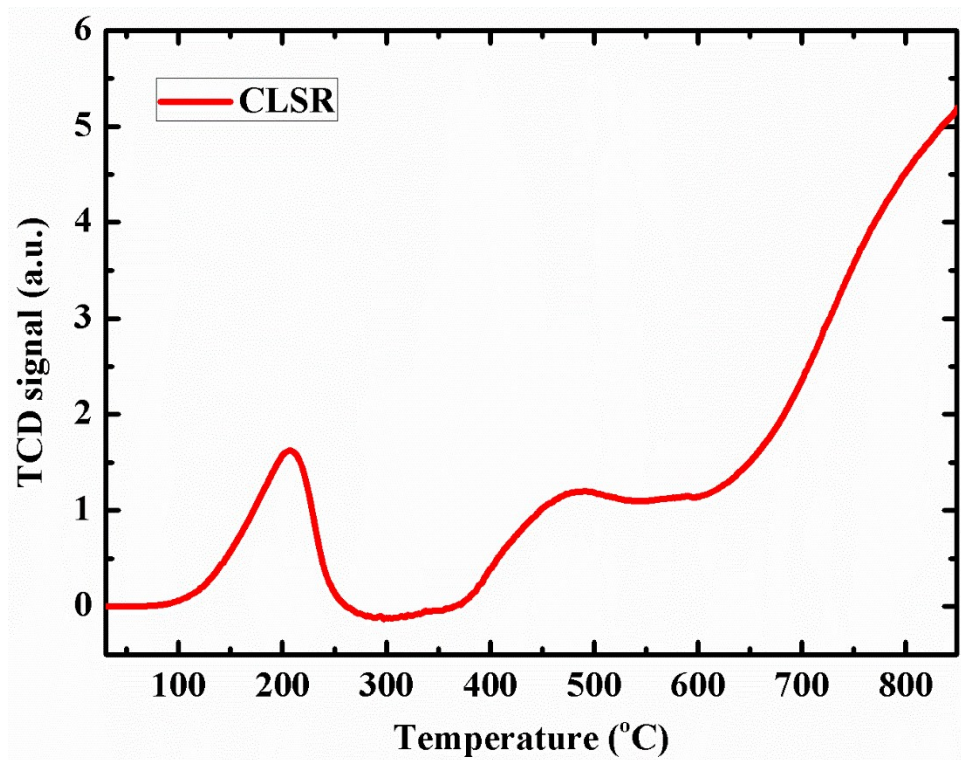


**Figure S6a:** Normalized XANES spectra of CLSR at Ruthenium K-edge along with the spectra of reference samples.

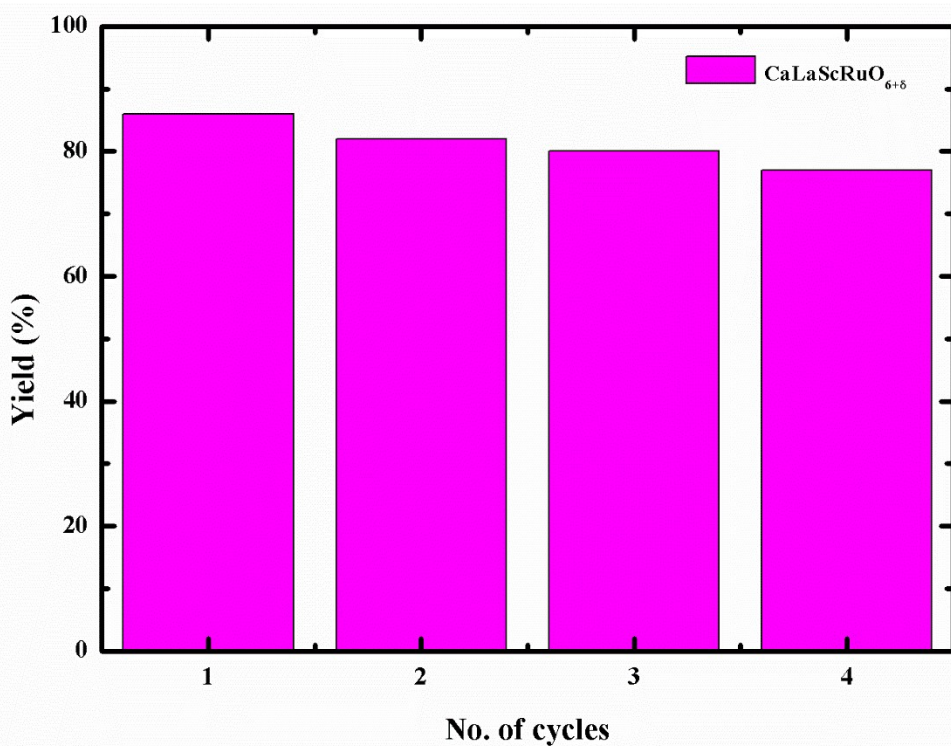
We have performed Ru K-edge XANES measurement to confirm the oxidation state of ruthenium by employing LCF fitting and the basic idea behind the LCF fitting is simple linear combination of two or more spectrum ( $Z = a^*X + b^*Y$ ). Since, if we want to produce our unknown spectrum from the standards, the best method is to use exact same coordination geometry of standards as it is present in the sample. Here, we used  $\text{Ca}_2\text{FeRuO}_6$  ( $\text{Ru}^{+5}$ ) had almost same coordination geometry. For +4 oxidation state, we have used  $\text{SrRuO}_3$  and  $\text{RuO}_2$  ( $\text{Ru}^{+4}$ ) and compared their fitting statistics as shown in figure below. It can be seen that all the spectral features at A (22129 eV), B (22140 eV) and C (22167 eV) present in +5 standard in the CLSR, which also establishes that +5 oxidation state is the major oxidation state of Ru in our material. This XANES profile of our material is also similar to that of  $\text{Ca}_2\text{YRuO}_6$  ( $\text{Ru}^{+5}$ ) as reported by Vitova *et. al.*, (Phys. Rev. B 89 (2014) 144112). As shown in Figure S6b, the LCF fittings are also carried with  $\text{SrRuO}_3$  and  $\text{RuO}_2$  as  $\text{Ru}^{+4}$  standards. The linear combination fitting using  $\text{SrRuO}_3$  standards shows 93% of  $\text{Ru}^{+5}$  oxidation state and 7 % of  $\text{Ru}^{+4}$  oxidation state. We would like to make a note here that, the fitting statistics of LCF fitting using  $\text{SrRuO}_3$  is relatively poor ( $R_{\text{factor}} = 0.73\%$ ) compared to LCF using  $\text{RuO}_2$  ( $R_{\text{factor}} = 0.67\%$ ) standard.



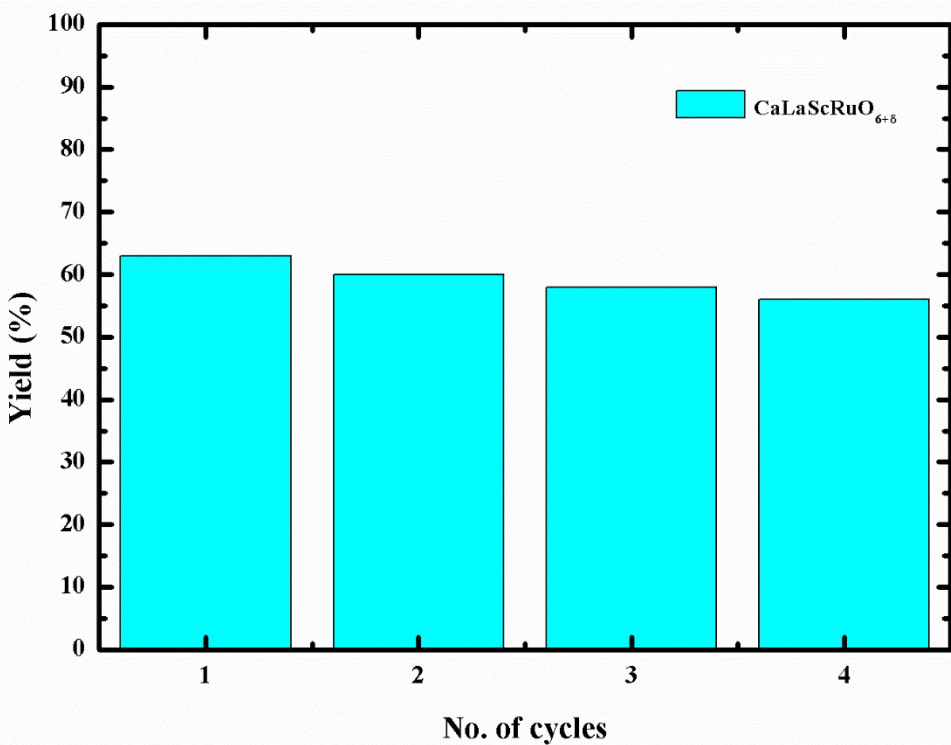
**Fig. S6b:** Linear combination fitting XANES spectrum of CLSR along with  $\text{Ca}_2\text{FeRuO}_6$  ( $\text{Ru}^{+5}$ ) and  $\text{SrRuO}_3$  ( $\text{Ru}^{+4}$ ) in upper section;  $\text{Ca}_2\text{FeRuO}_6$  ( $\text{Ru}^{+5}$ ) and  $\text{RuO}_2$  ( $\text{Ru}^{+4}$ ) as reference in lower section.



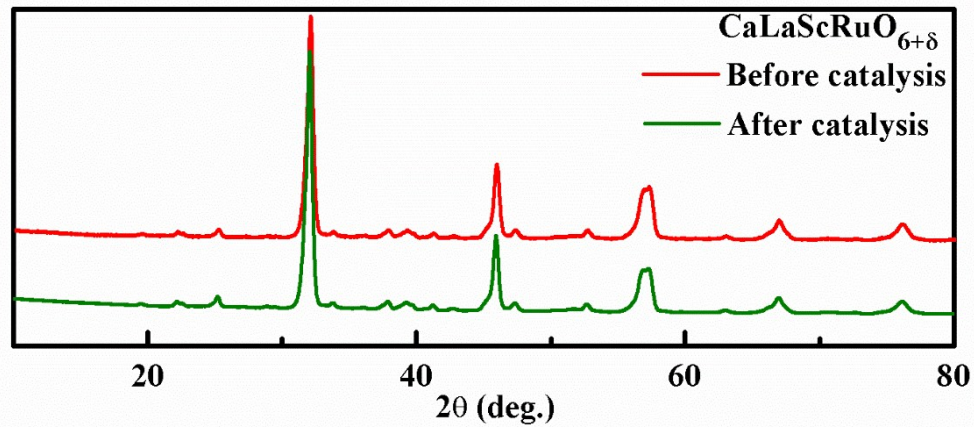
**Figure S7:** H<sub>2</sub>-TPR curve as a function of temperature.



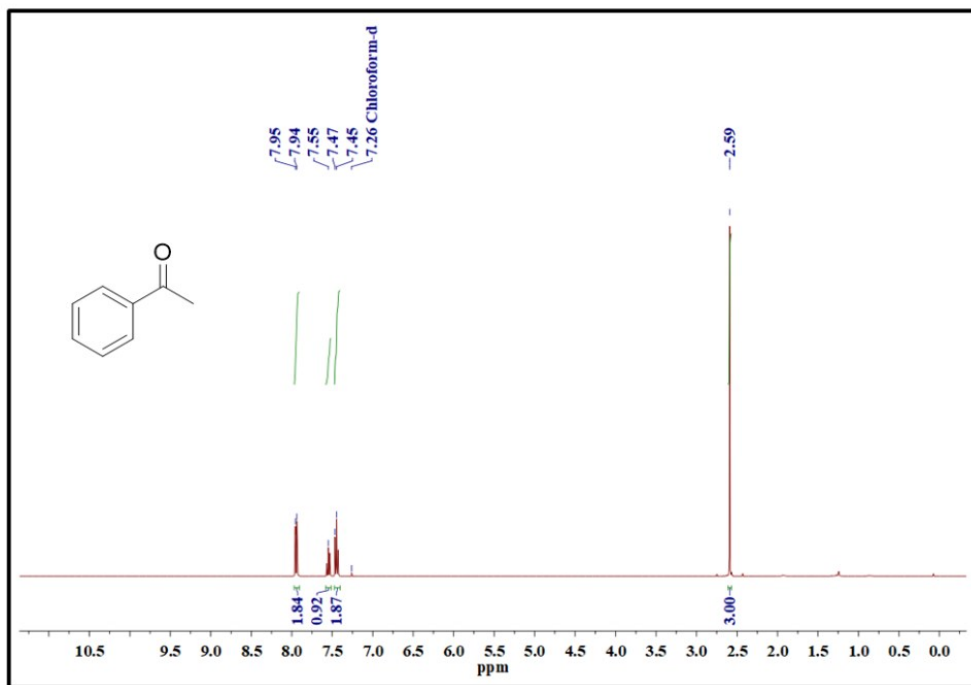
**Figure S8:** Recyclability experiments up to next 4 consecutive cycles for the formation of benzaldehyde



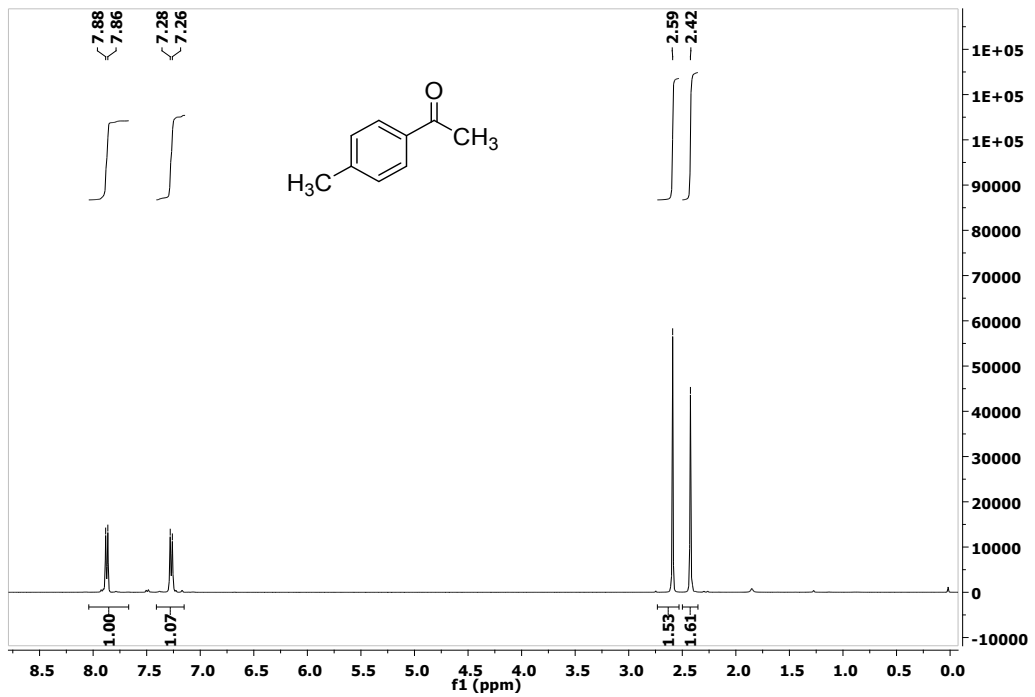
**Figure S9:** Recyclability experiments up to next 4 consecutive cycles for the formation of  $\gamma$ -Butyrolactone.



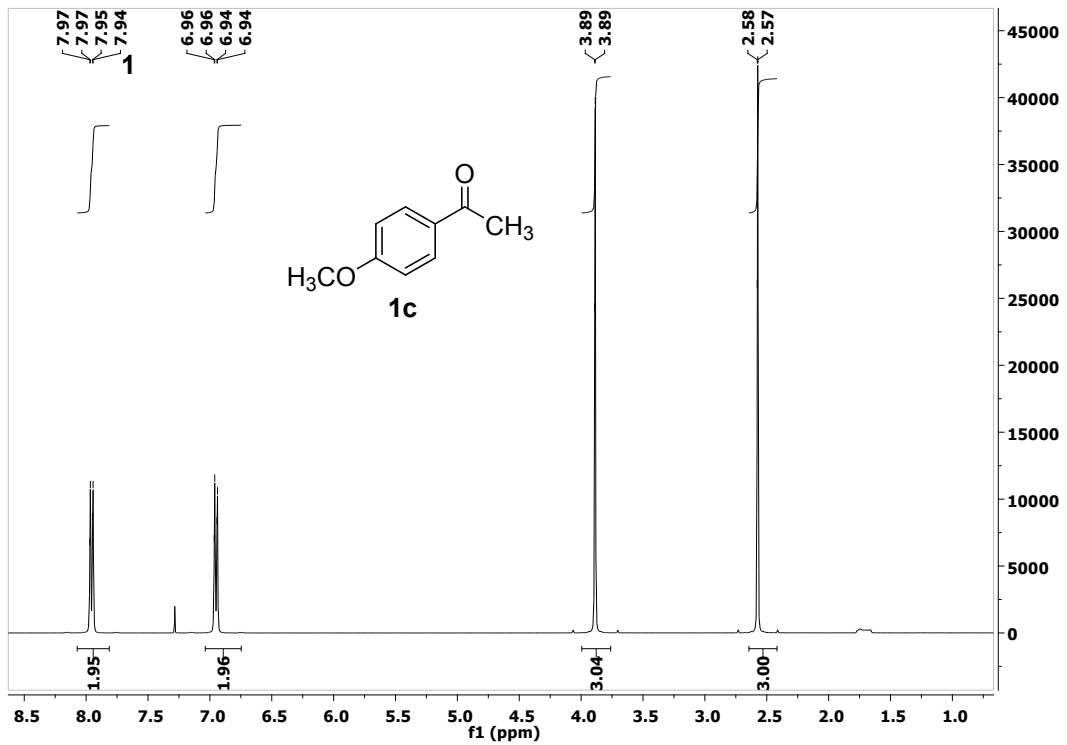
**Figure S10:** PXRD pattern showing the similar structural behavior before and after the catalysis.



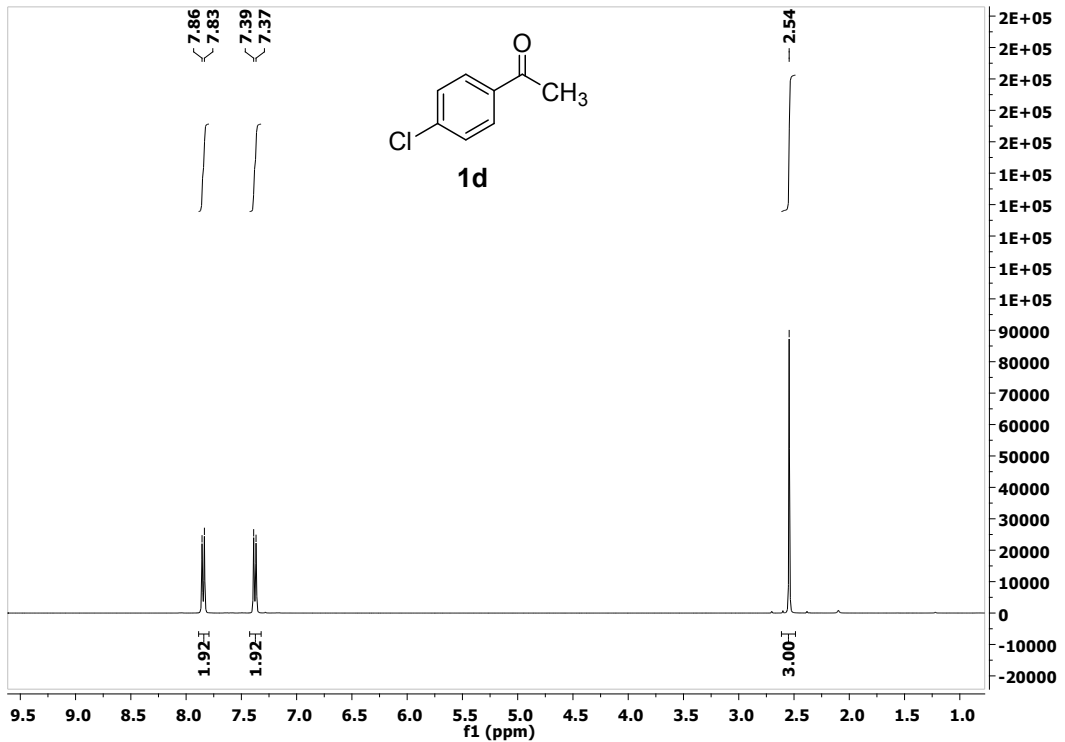
**Figure S11:** <sup>1</sup>H-NMR spectrum of acetophenone (1a).



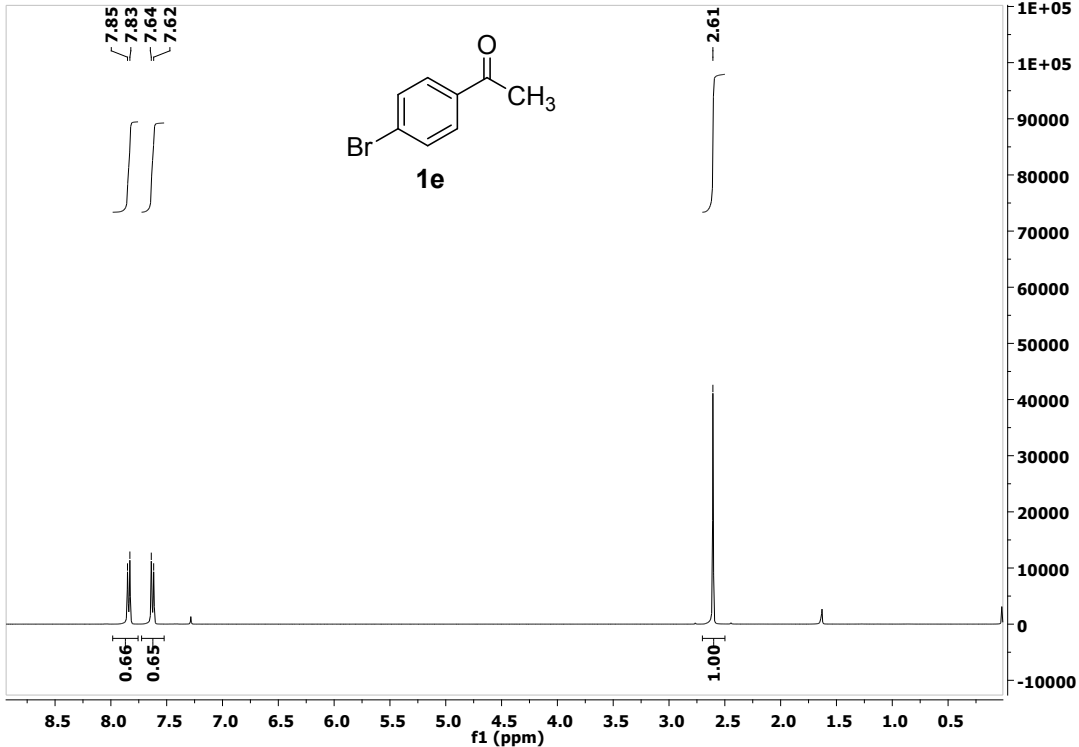
**Figure S12:**  $^1\text{H}$ -NMR spectrum of 1b.



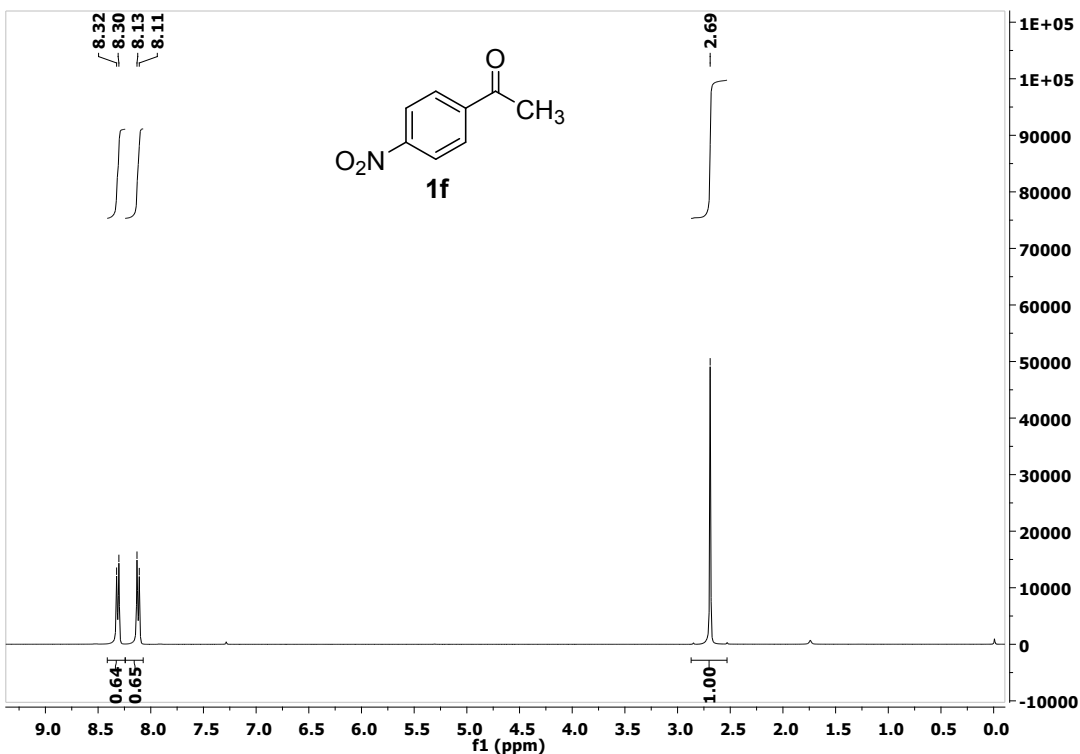
**Figure S13:**  $^1\text{H}$ -NMR spectrum of 1c.



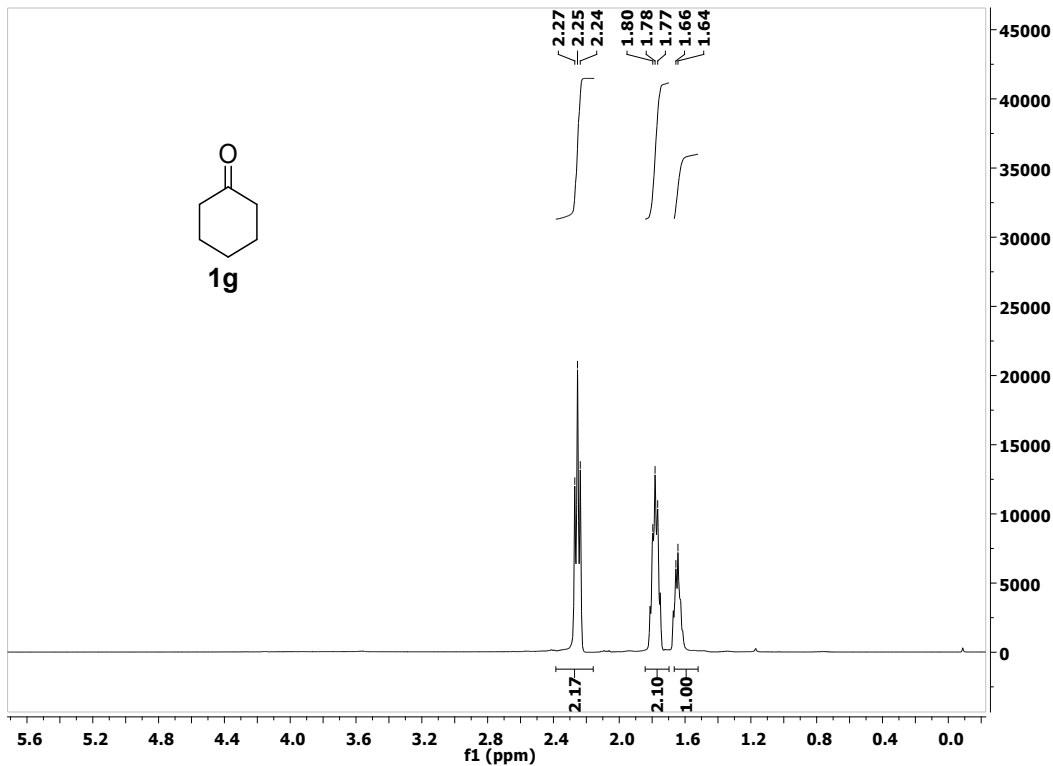
**Figure S14:**  $^1\text{H}$ -NMR spectrum of **1d**.



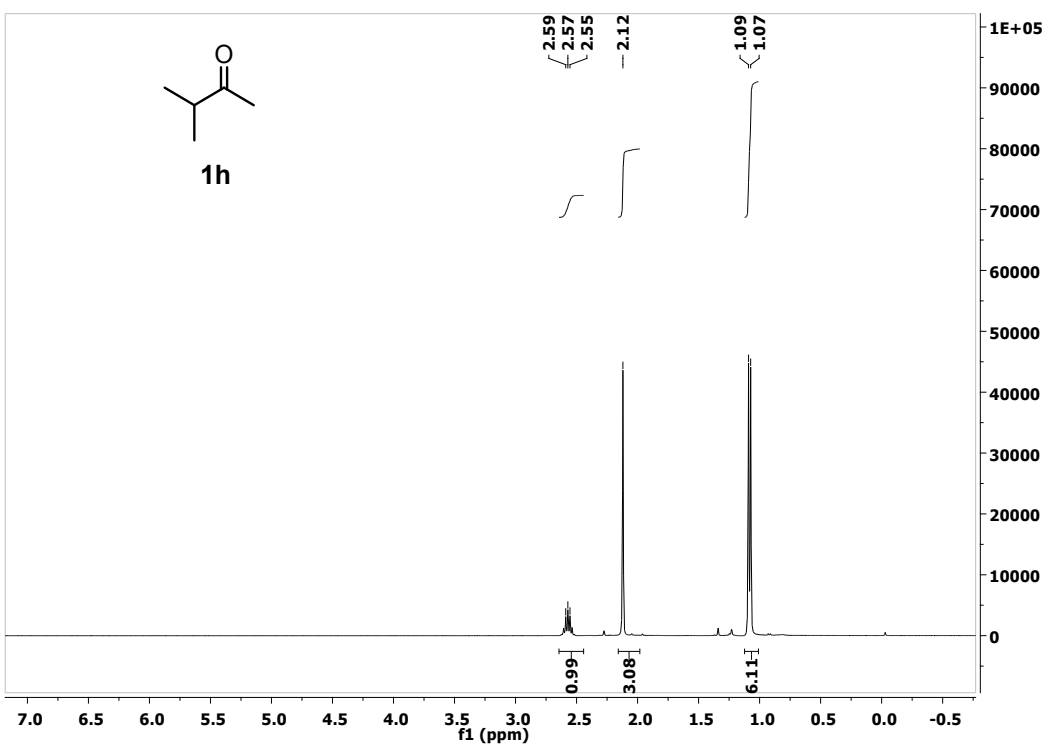
**Figure S15:**  $^1\text{H}$ -NMR spectrum of **1e**.



**Figure S16:**  $^1\text{H}$ -NMR spectrum of **1f**.



**Figure S17:**  $^1\text{H}$ -NMR spectrum of **1g**.



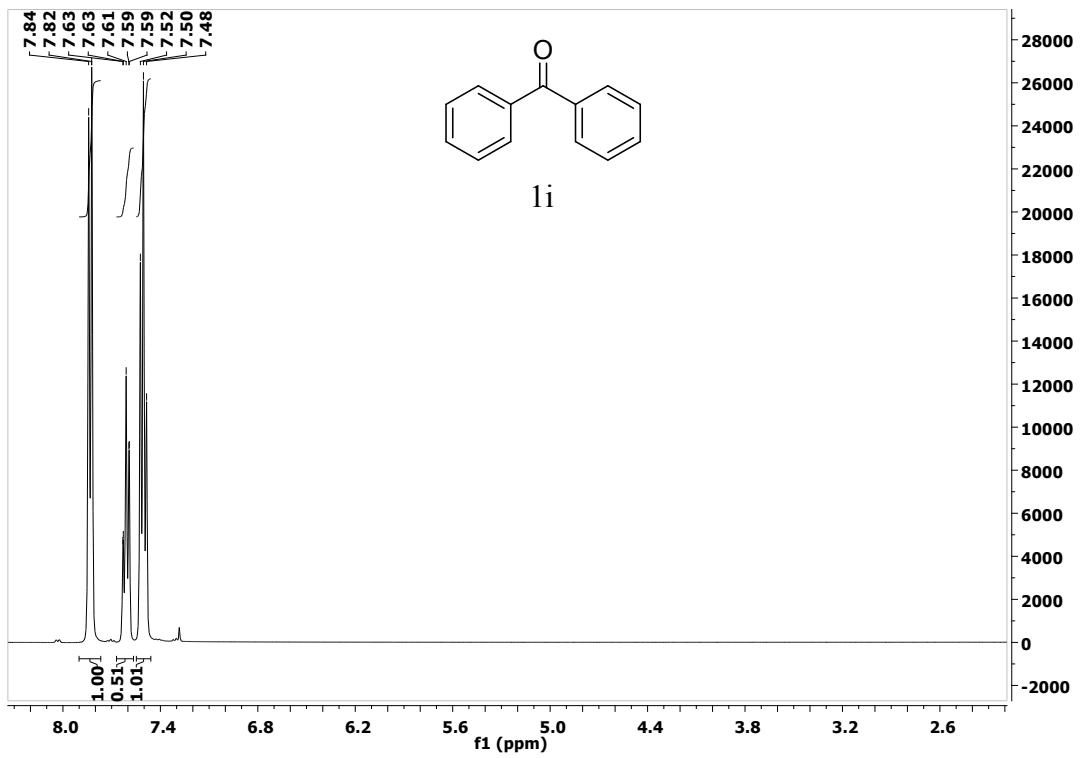


**Figure S19:**  $^1\text{H}$ -NMR spectrum of  $1\text{i}$ .

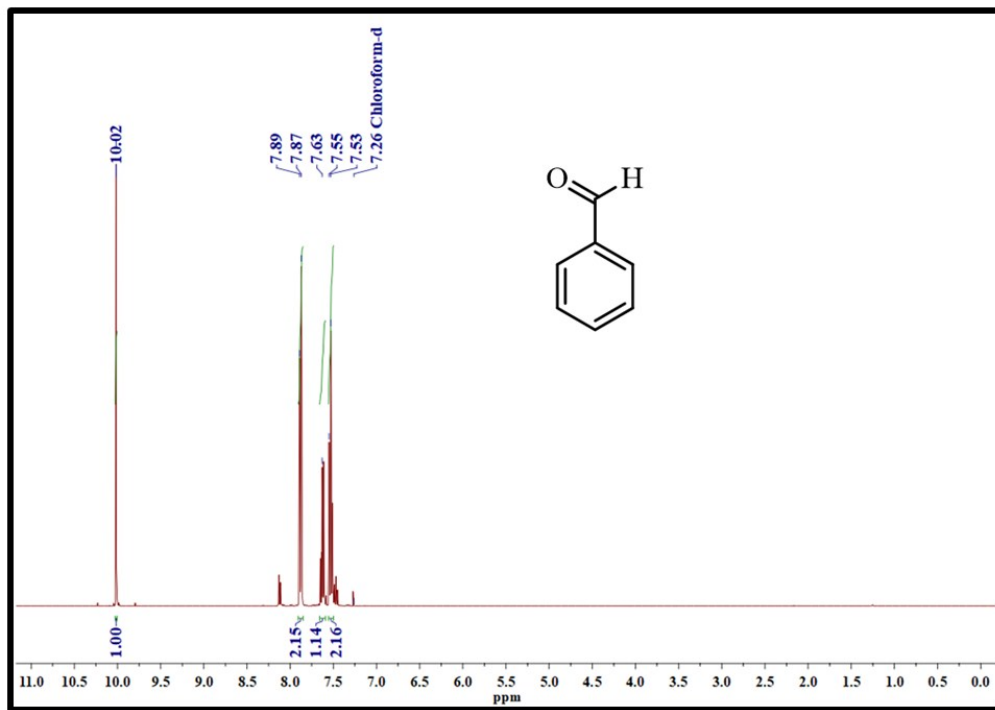


**Figure S20:** <sup>1</sup>H-NMR spectrum of benzaldehyde (2a).

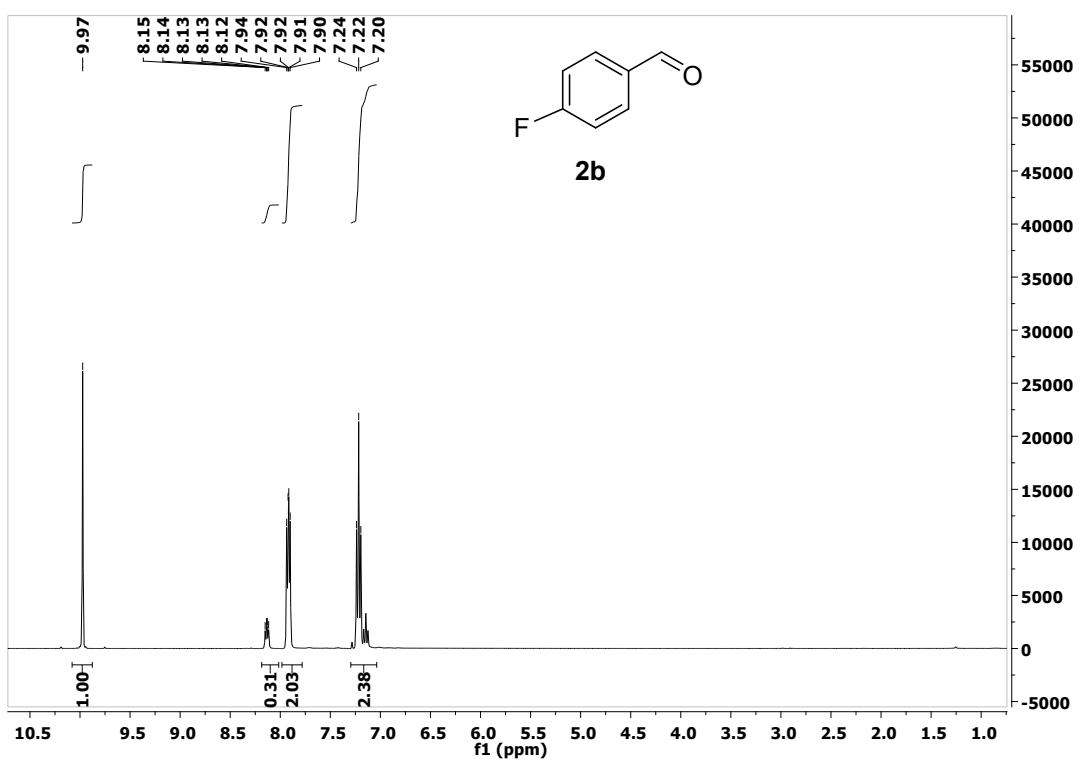


**Figure S21:** <sup>1</sup>H-NMR spectrum of 2b.

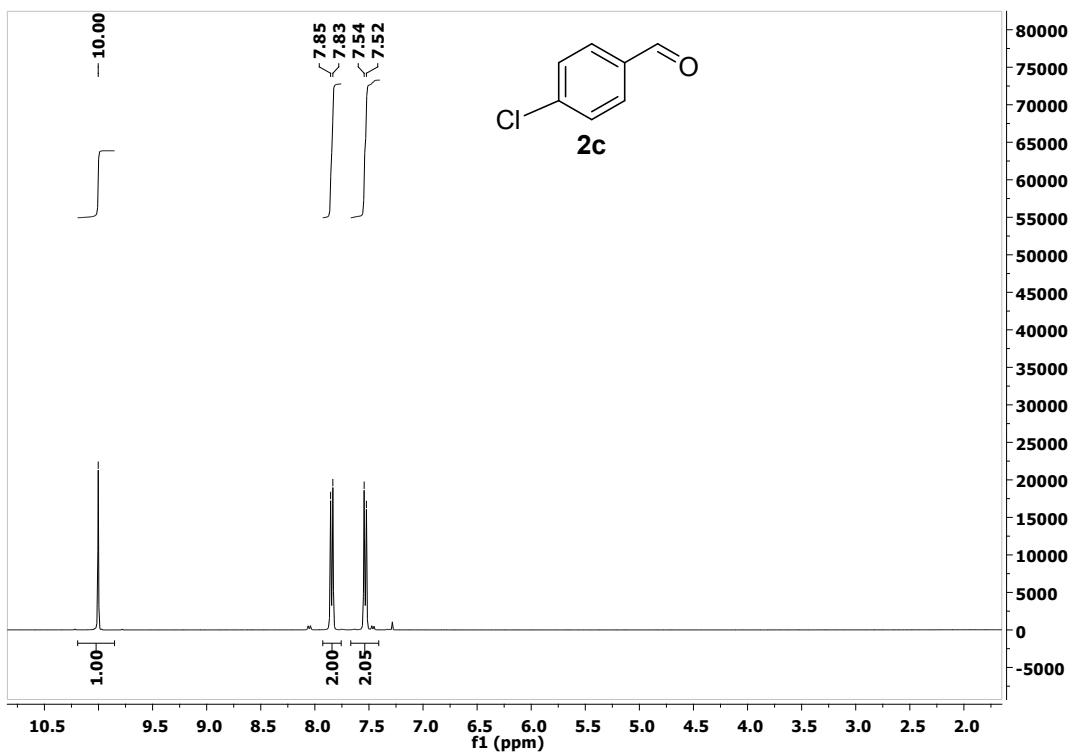


**Figure S22:**  $^1\text{H}$ -NMR spectrum of **2c**.

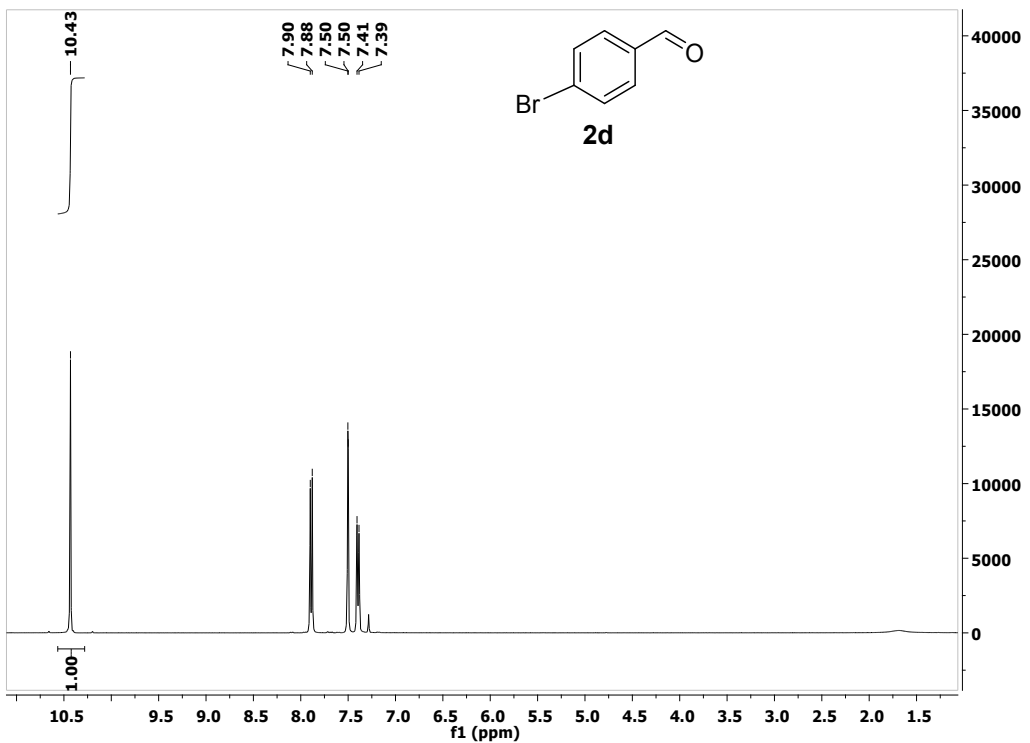


**Figure S23:** <sup>1</sup>H-NMR spectrum of **2d**.

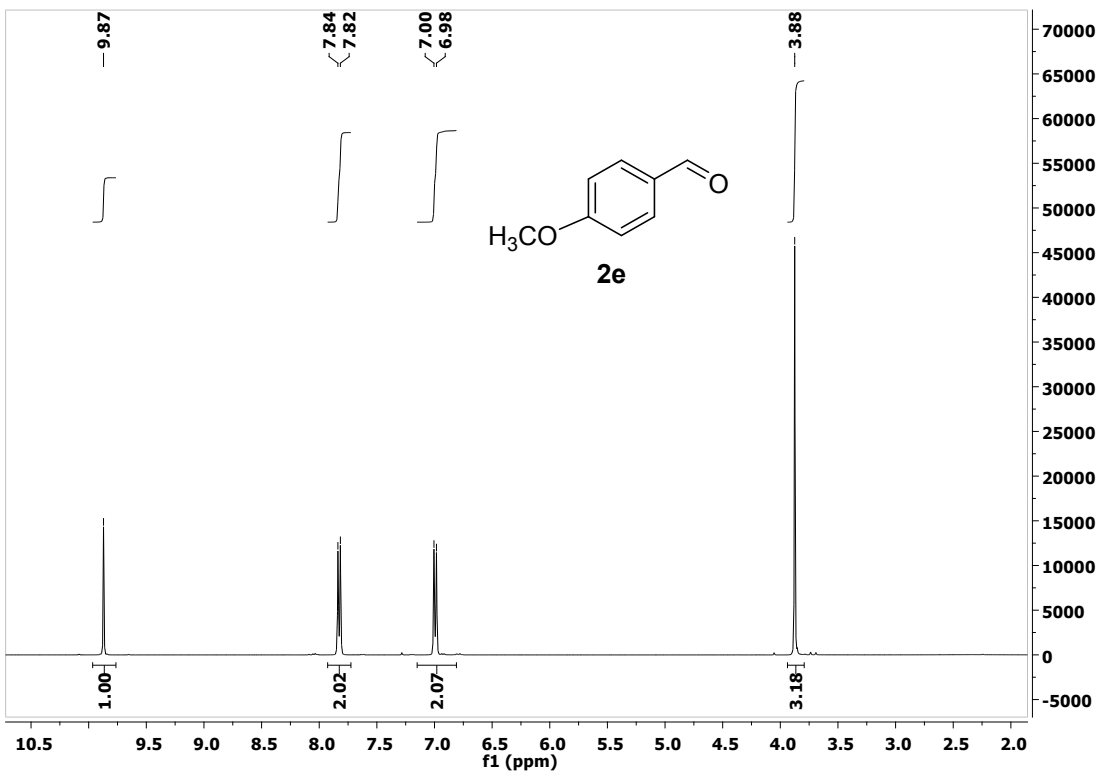


**Figure S24** <sup>1</sup>H-NMR spectrum of **2e**.

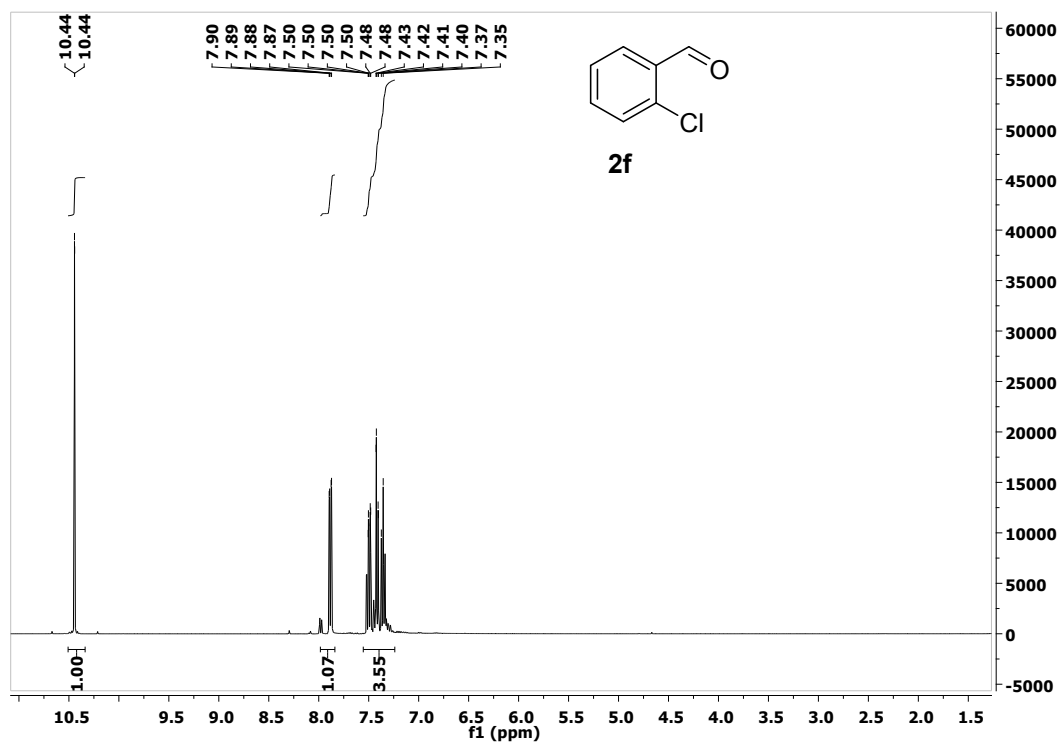


**Figure S25:**  $^1\text{H}$ -NMR spectrum of 2f.

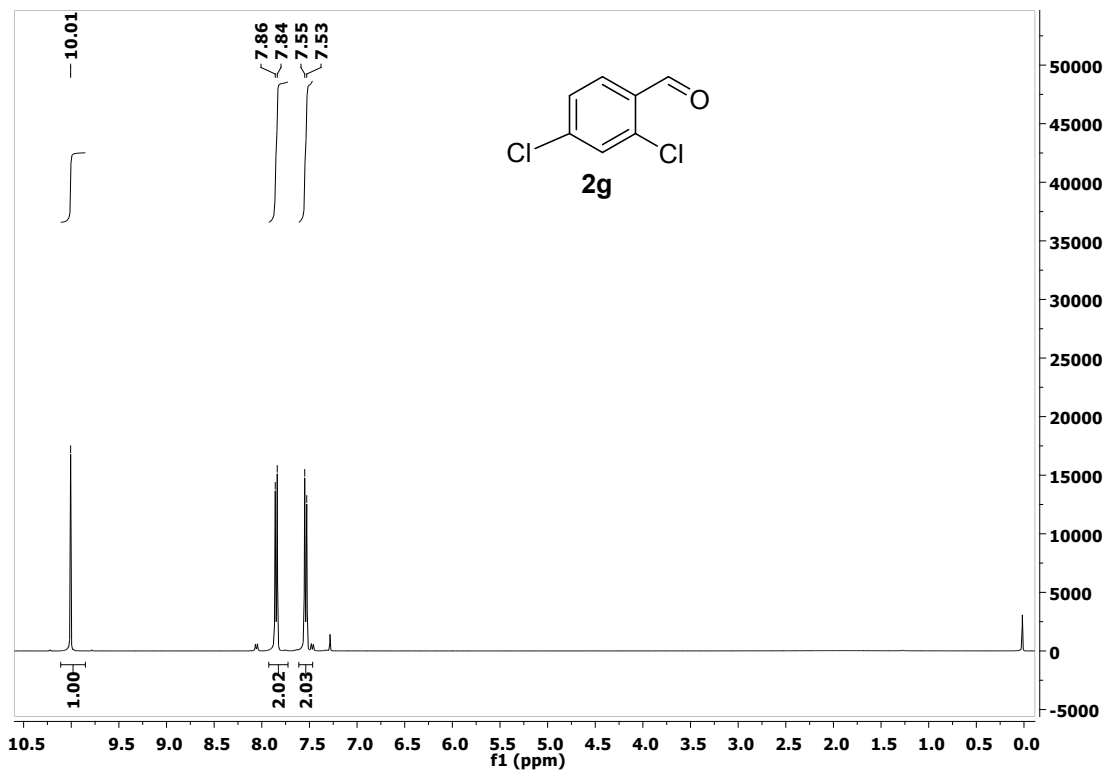


**Figure S26:** <sup>1</sup>H-NMR spectrum of 2g.

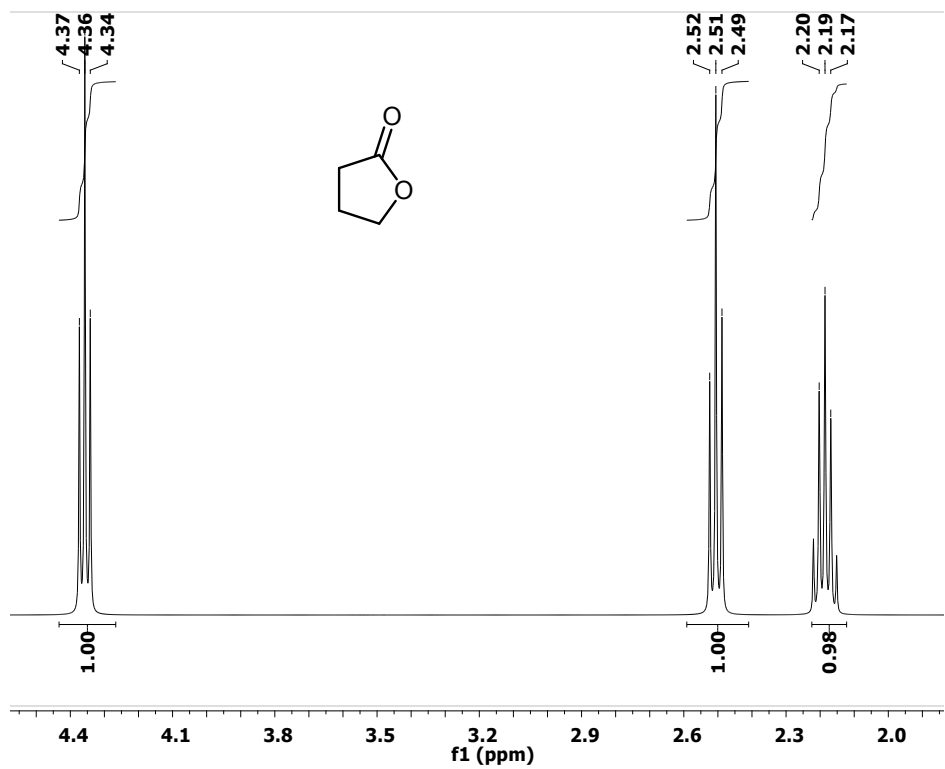


**Fig S27:** <sup>1</sup>H-NMR spectrum of 3a

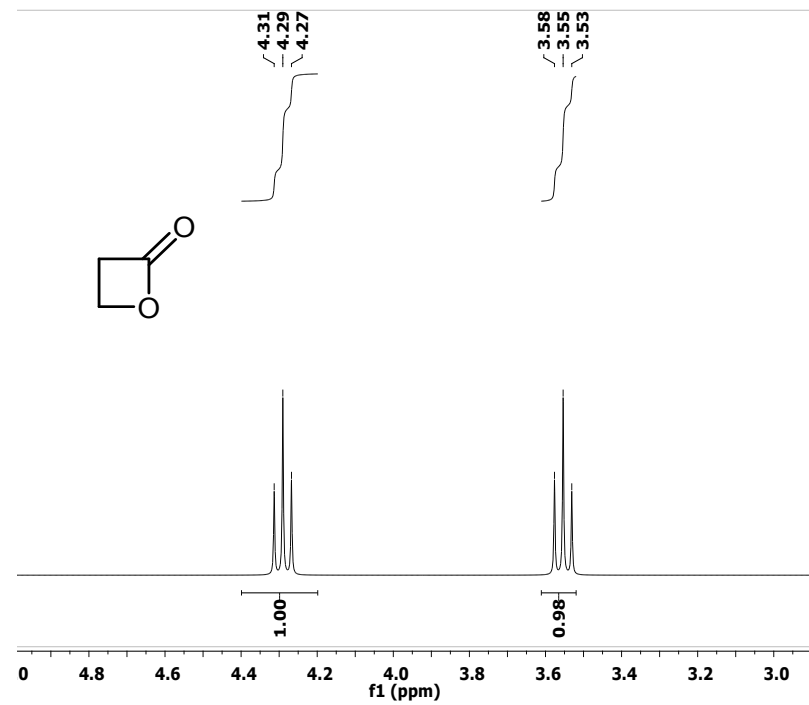


**Figure S28:**  $^1\text{H}$ -NMR spectrum of 3b.

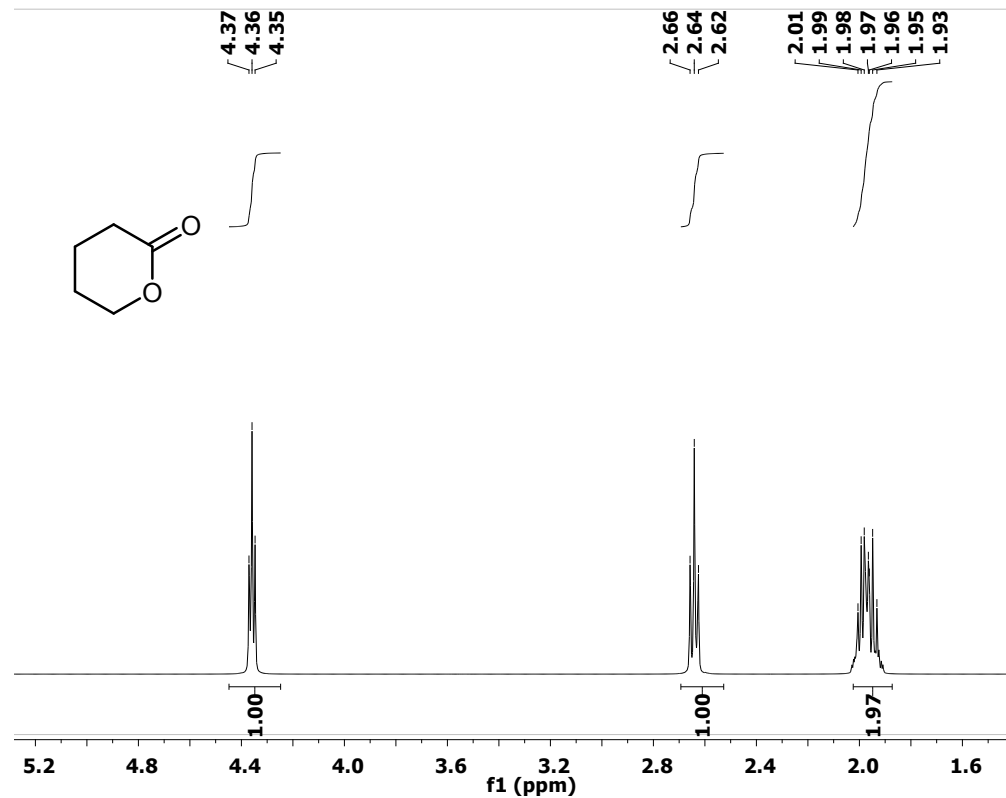


**Figure S29:**  $^1\text{H}$ -NMR spectrum of 3c.

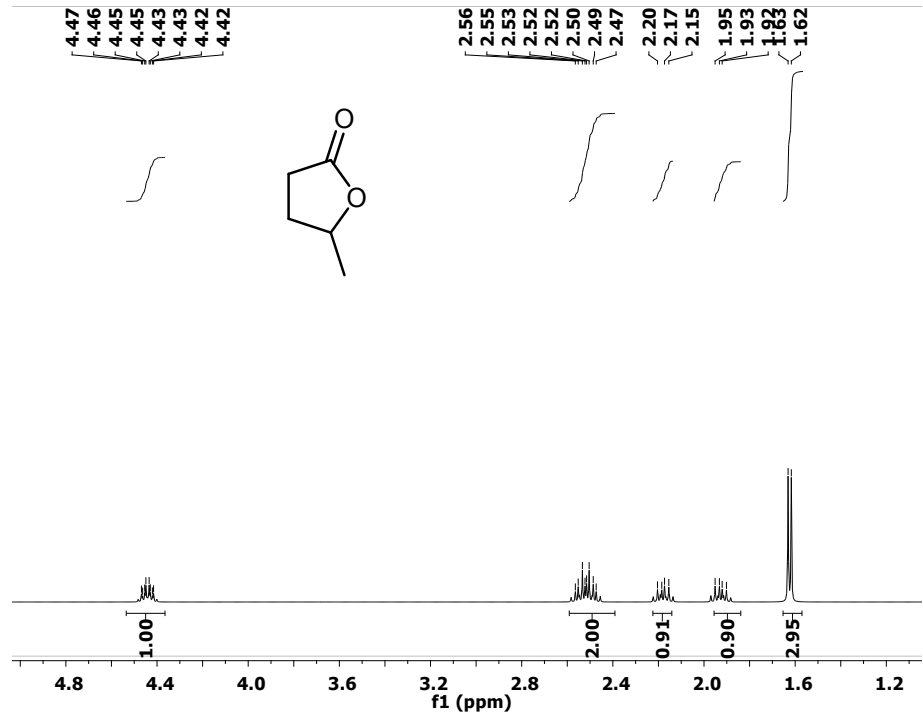


**Figure S30:**  $^1\text{H}$ -NMR spectrum of 3d.

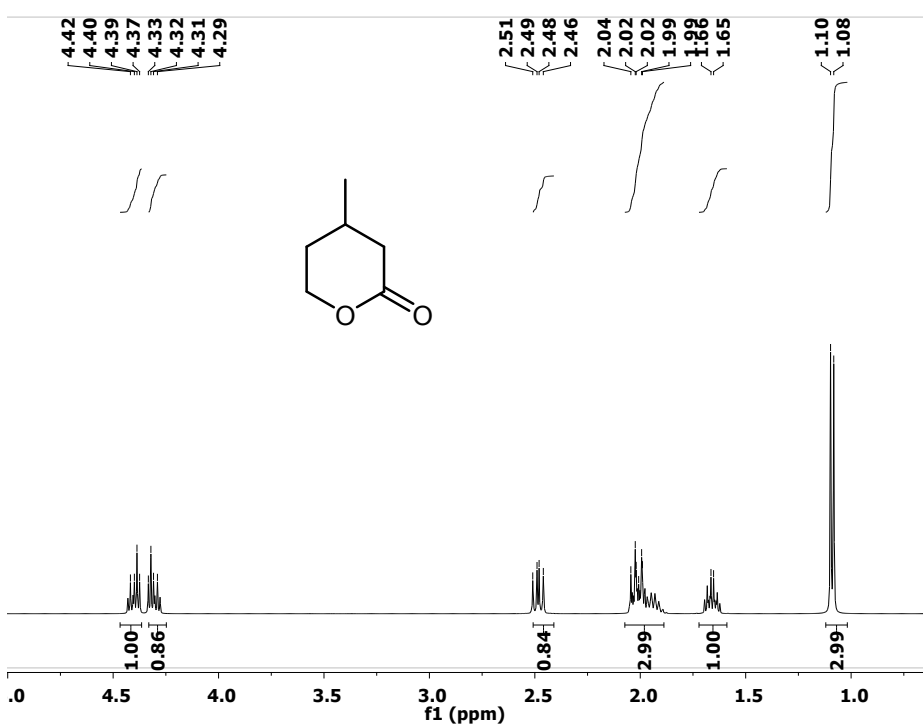


**Figure S31:**  $^1\text{H}$ -NMR spectrum of 3e.

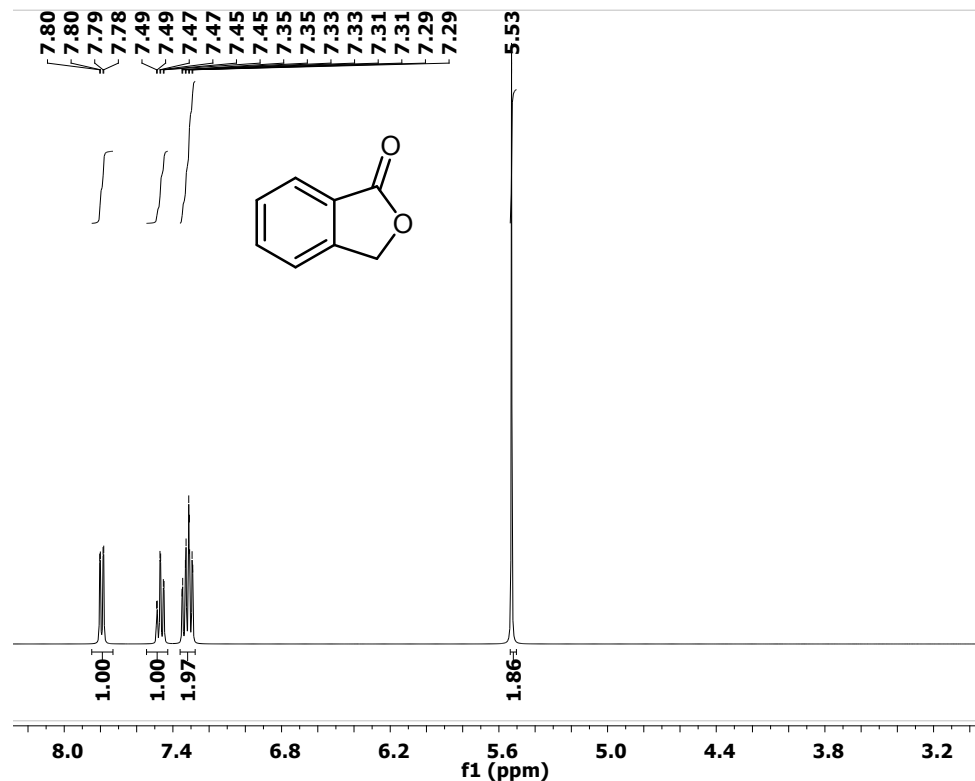


Figure S32: <sup>1</sup>H-NMR spectrum of 3f.

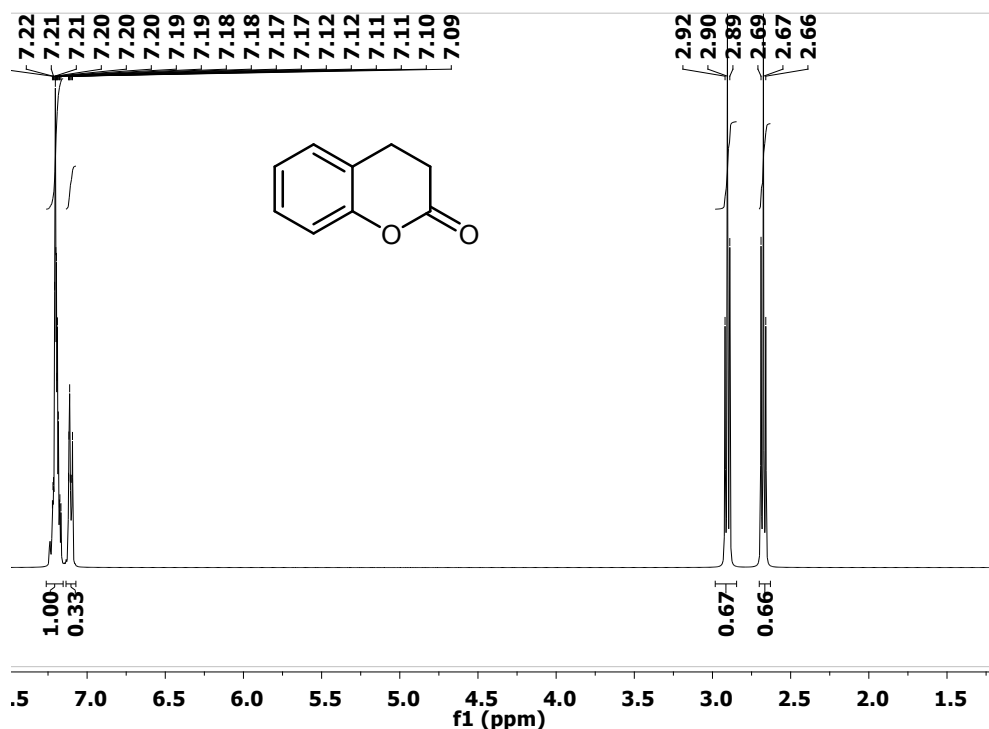
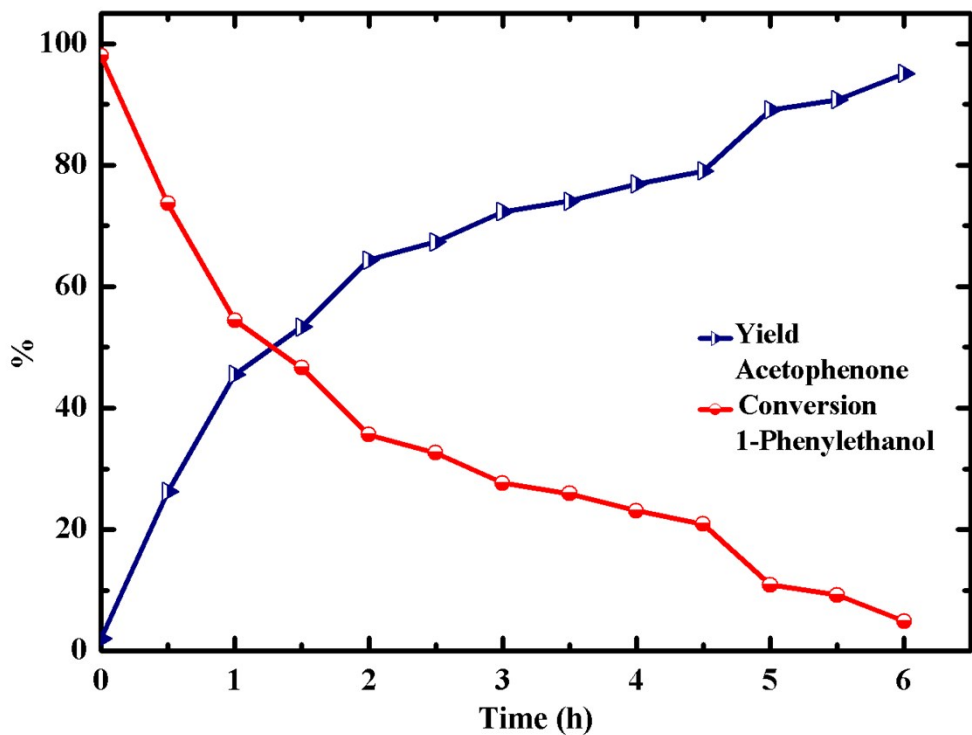
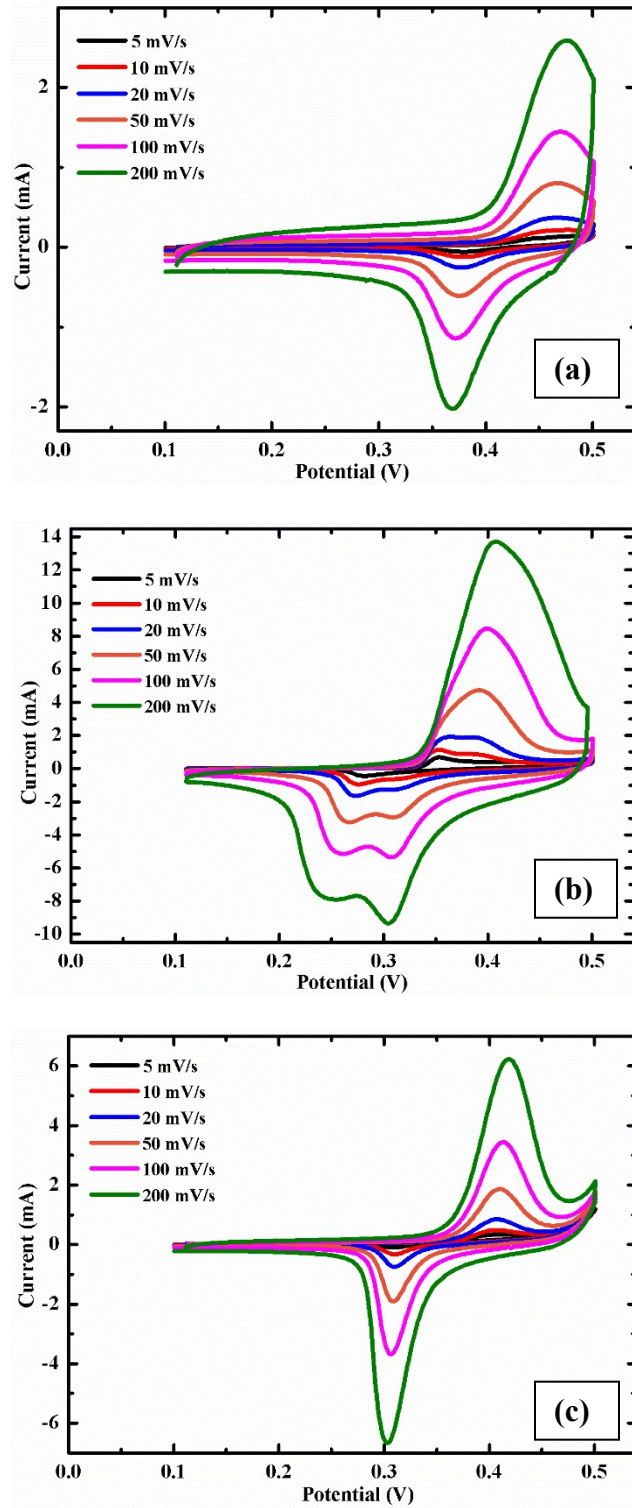


Figure S33: <sup>1</sup>H-NMR spectrum of 3g.



**Figure S34:** Time dependent yields and remaining starting material during the conversion of 1 to 1a by using catalyst (CLSR).



**Figure S35:** Cyclic voltammograms at different scan rates in (a) 2M KOH (b) 4M KOH and (c) 6M KOH as electrolyte.

## References:

- (1) Poswal, A. K.; Agrawal, A.; Yadav, A. K.; Nayak, C.; Basu, S.; Kane, S. R.; Garg, C. K.; Bhattachryya, D.; Jha, S. N.; Sahoo, N. K. Commissioning and First Results of Scanning Type EXAFS Beamline (BL-09) at INDUS-2 Synchrotron Source. *AIP Conference Proceedings*. **2014**, *1591*, 649–651.
- (2) Basu, S.; Nayak, C.; Yadav, A. K.; Agrawal, A.; Poswal, A. K.; Bhattachryya, D.; Jha, S. N.; Sahoo, N. K., A comprehensive facility for EXAFS measurements at the INDUS-2 synchrotron source at RRCAT, Indore, India. *J. Phys. Conf. Ser.* **2014**, *493* (1), 012032 (1-4).
- (3) Serpil Gönen, Z.; Gopalakrishnan, J.; Eichhorn, B.W.; Ferrimagnetism and metal–insulator transitions in the  $\text{LaMnxRu}_{1-x}\text{O}_3$  perovskites. *Solid State Sci.* **2002**, *4*, 773–778.
- (4) Dass, R. I.; Yan, J.-Q.; Goodenough, J. B., Oxygen stoichiometry, ferromagnetism and transport properties of  $\text{La}_{2-x}\text{NiMnO}_{6+\delta}$  *Phys. Rev. B*, **2003**, *68*, 064415 (1-12).
- (5) Kawasaki, S.; Kamata, K.; Hara, M. Dioxygen Activation by a Hexagonal  $\text{SrMnO}_3$  Perovskite Catalyst for Aerobic Liquid-Phase Oxidation. *ChemCatChem* **2016**, *8* (20), 3247–3253.
- (6) Bhatia, A.; Muthaiah, S. K. Well-Defined Ruthenium Complex for Acceptorless Alcohol Dehydrogenation in Aqueous Medium. *Chemselect*. **2018**, *3* (13), 3737-3741.
- (7) Bhatia, A.; Muthaiah, S. K.; Kannan, M.K. Ruthenium-Promoted Acceptorless and Oxidant-Free Lactone Synthesis in Aqueous Medium, *Chemselect*. **2019**, *30*, 721-725.
- (8) Wilde, P. M.; Guther, T. J.; Oesten, R.; Garche, J. Strontium Ruthenate Perovskite as the Active Material for Supercapacitors. *J. Electroanal. Chem.* **1999**, *461* (1–2), 154–160.
- (9) Alam, M.; Karmakar, K.; Pal, M.; Mandal, K. Electrochemical Supercapacitor Based on Double Perovskite  $\text{Y}_2\text{NiMnO}_6$  Nanowires. *RSC Adv.* **2016**, *6* (115), 114722–114726.